



Forschungszentrum Karlsruhe
Technik und Umwelt

Wissenschaftliche Berichte
FZKA 5808

**ITER ECH Window
Development
Final Report**

**M. Thumm, O. Braz, H. E. Häfner,
R. Heidinger, A. Möbius, P. Norajitra,
G. Soudée**

**Institut für Technische Physik
Institut für Materialforschung
Projekt Kernfusion**

September 1996

Forschungszentrum Karlsruhe
Technik und Umwelt
Wissenschaftliche Berichte
FZKA 5808

ITER ECH Window Development
- Final Report -

M. Thumm, O. Braz, H. E. Häfner, R. Heidinger, A. Möbius*,
P. Norajitra, G. Soudée

Institut für Technische Physik
Institut für Materialforschung
Projekt Kernfusion

*IMT GmbH, Luisenstr. 23, D-76344 Eggenstein, Germany

Forschungszentrum Karlsruhe GmbH, Karlsruhe

1996

**Als Manuskript gedruckt
Für diesen Bericht behalten wir uns alle Rechte vor**

**Forschungszentrum Karlsruhe GmbH
Postfach 3640, 76021 Karlsruhe**

ISSN 0947-8620

ITER ECH WINDOW DEVELOPMENT

- Final Report -

Task No.: G52TT07 94-08-03FE

ID No.: T25

Abstract

In a high power experiment using a Russian 140 GHz, 0.5 MW, 1 s gyrotron the power absorbed in a circular, liquid nitrogen edge cooled, single-disk sapphire window (HEMEX) was determined. Within the experimental uncertainties, the measured loss tangent values of $(8 \pm 4) \times 10^{-6}$ in the temperature range between 87 and 95 K are in good agreement with cold test measurements.

The assessment of a medium aspect ratio elongated liquid nitrogen edge cooled, single-disk sapphire window has shown, that the use of an elliptical rf beam with flattened power distribution and an aspect ratio of 8:1 (252 mm x 32 mm window aperture) or of a ring-shaped elliptical beam with an aspect ratio of 3:1 (156 mm x 52 mm) allows a power transmission capability of 1 MW, CW at 170 GHz. Finite element calculations on stress distribution at 5 bar overpressure show that all stresses are well below the admissible limits. A principle design of the window assembly is presented.

Finite element calculations on a liquid neon edge cooled, single-disk sapphire window using pessimistic values of loss tangent and thermal conductivity give a CW power transmission capability for a Gaussian/HE₁₁-power distribution of 2.8 MW, 2.3 MW and 1.8 MW at 140 GHz, 170 GHz and 220 GHz, respectively, allowing even 2 MW, CW windows at 170 GHz. Calculations on stress distribution (5 bar overpressure) and a final principle design were done.

Finite element calculations on a large aspect ratio rectangular Brewster window (680 mm x 12 mm) with water edge cooling at 293 K show that Au-doped silicon and PACVD diamond are possible candidates for CW operation around 170 GHz. Diamond is preferable since there is no danger of enhanced losses due to thermal excitation of charge carriers at temperatures higher than 350 K. The final design of the window assembly is presented. The total losses of the assembly (7.3 %) can be reduced to approximately 3 % by using periodically rippled wall mode converters to generate the 90 % HE₁₁/10 % HE₁₂ (in phase) mode mixture for optimum coupling to the free-space Gaussian mode.

ITER ECH FENSTERENTWICKLUNG

-Schlußbericht -

Task No.: G52TT07 94-08-03FE
ID No.: T25

Kurzfassung

In einem Hochleistungsexperiment mit einem russischen 140 GHz, 0,5 MW, 1s Gyrotron wurde die in einer runden, mit flüssigem Stickstoff am Rand gekühlten Saphirscheibe (HEMEX) absorbierte Leistung bestimmt. Innerhalb der experimentellen Unsicherheiten stimmen die im Temperaturbereich zwischen 87 und 95 K gemessenen Verlusttangenswerte vom $(8 \pm 4) \times 10^{-6}$ gut mit Niederleistungsmessungen überein.

Die theoretische Analyse eines elongierten, mit flüssigem Stickstoff am Rand gekühlten Einscheibensaphirfensters hat ergeben, daß bei Verwendung eines elliptischen HF-Strahls mit abgeflachter Leistungsverteilung das Aspektverhältnis von 8:1 (252 mm x 32 mm Fensteröffnung) oder bei einem ringförmigen elliptischen Strahl das Aspektverhältnis von 3:1 (156 mm x 52 mm Fensteröffnung) ein Leistungstransmissionsvermögen von 1 MW CW bei 170 GHz erlaubt. Finite-Element-Berechnungen der Verteilung mechanischer Spannungen bei 5 bar Überdruck zeigen, daß alle Werte weit unterhalb der zulässigen Grenzwerte liegen. Eine Prinzipauslegung der Fensteranordnung wurde erstellt.

Finite-Element-Rechnungen zu einem mit flüssigem Neon am Rand gekühlten Einscheibensaphirfensters unter Verwendung pessimistischer Werte für den Verlusttangens und die Wärmeleitfähigkeit ergeben Leistungstransmissionskapazitäten bei Gaußscher- bzw. HE_{11} -Leistungsverteilung von 2,8 MW, 2,3 MW und 1,8 MW bei 140 GHz, 170 GHz und 220 GHz. Berechnungen der Verteilung mechanischer Spannungen bei 5 bar Überdruck und eine Prinzipauslegung des Fensters wurden durchgeführt.

Finite-Element-Rechnungen zu einem stark elongierten, rechteckigen Brewster-Fenster (680 mm x 12 mm) mit Wasserrandkühlung bis 293 K haben ergeben, daß gold-dotiertes Silizium und PACVD Diamant für 170 GHz, CW Betrieb geeignet sind. Diamant ist vorzuziehen, da bei Temperaturen höher als 350 K keine Gefahr thermischer Freisetzung von Ladungsträgern besteht. Eine Auslegung der Fensteranordnung wurde erstellt. Die Gesamtverluste der Anordnung (7,3 %) können auf etwa 3 % reduziert werden, wenn Wellentypwandler mit periodisch gestörter Wand eingesetzt werden, um eine 90 % HE_{11} /10 % HE_{12} -Modenmischung (in Phase) zur optimalen Kopplung an die Freiraum-Gauß-Mode herzustellen.

Contents

	Summary	3
1.	Introduction and Present Status of Experiments	4
2.	Material Characterization, Selection and Concepts	5
2.1	Water Cooled Windows ($T_0 = 293$ K)	5
2.1.1	Distributed Sapphire Window	5
2.1.2	PACVD-Diamond Window (Edge Cooled)	5
2.1.3	Au-Doped Silicon Window (Edge Cooled)	8
2.1.4	Large-Aspect-Ratio Rectangular Brewster Window	8
2.2.	CHF ₃ or CF ₃ Cl Edge-Cooled Windows ($T_0 \leq 200$ K)	8
2.3	Liquid Nitrogen Edge-Cooled Windows ($T_0=77$ K)	8
2.3.1	Sapphire Window	8
2.3.2	Au-doped Silicon Window	9
2.4	Cryogenic Sapphire Window at $T_0=20-30$ K	9
3.	Potential Options	10
4.	Performance Targets and Development Strategy	10
5.	Subtask 1: High power experiment (140 GHz, 0.5 MW, 1s) for determination of the power absorbed in a liquid nitrogen edge cooled single disk sapphire circular window (high power window calorimeter). Validation of the parameters of sapphire	13
5.1	Experimental Method	14
5.2	Experimental Arrangement	16
5.3	Experimental Results and Conclusions	18
6.	Subtask 2: Assessment and design of a medium aspect ratio rectangular liquid nitrogen edge cooled single disk sapphire window for 170 GHz, 1 MW, CW operation	21
6.1	Concept of Elongated Sapphire Window	22
6.2	Calculation of Power Capabilities	24
6.3	Analytical Calculations on Stress Distributions	24
6.4	Numerical Calculations on Stress Distributions	27
6.5	Production and Metallization of Elongated Sapphire Disks	30
7.	Subtask 3: Assessment and design of a non-cryogenic, large-aspect-ratio rectangular, water-cooled single disk torus window system	31
7.1	Concept of Large-Aspect-Ratio Brewster Window	32
7.2	Quasi-optical Circular Corrugated (CC) to Rectangular Corrugated (RC) Waveguide Transition	34
7.3	Additional Losses	34
7.4	Large-aspect Ratio Rectangular Brewster window (57:1)	34
7.5	Conclusions	36
8.	Subtask 4: Optimization and design of a liquid neon edge cooled single disk sapphire window for 1 MW, CW operation	37
8.1	Concept of Liquid Neon Edge Cooled Single Disk Sapphire Window	38
8.2	Calculation of Power Transmission Capability	38
8.3	Preparation of an Experimental Validation (T245/6)	40
	References	42

Executive Summary

In a high power experiment using a Russian 140 GHz, 0.5 MW, 1 s gyrotron the power absorbed in a circular, liquid nitrogen edge cooled, single-disk sapphire window (HEMEX) was determined. Within the experimental uncertainties, the measured loss tangent values of $(8 \pm 4) \times 10^{-6}$ in the temperature range between 87 and 95 K are in good agreement with cold test measurements. Owing to a special nitrogen gas flushing system the window calorimeter could be operated at air pressure with only minor freezing and no rf arcing problems during a whole working day.

The assessment of a medium aspect ratio elongated liquid nitrogen edge cooled, single-disk sapphire window has shown, that the use of an elliptical rf beam with flattened power distribution and an aspect ratio of 8:1 (252 mm x 32 mm window aperture) or of a ring-shaped elliptical beam with an aspect ratio of 3:1 (156 mm x 52 mm) allows a power transmission capability of 1 MW, CW at 170 GHz. Finite element calculations on stress distribution at 5 bar overpressure show that all stresses are well below the admissible limits. Detailed computations employing a realistic brazing collar geometry and a principle design were done. In the case of the torus window a cold trap on the torus side should pump the dust in the waveguide.

Finite element calculations on a liquid neon edge cooled, single-disk sapphire window using pessimistic values of loss tangent and thermal conductivity show a CW power transmission capability for a Gaussian/ HE_{11} -power distribution of 2.8 MW, 2.3 MW and 1.8 MW at 140 GHz, 170 GHz and 220 GHz, respectively, allowing even 2 MW, CW windows at 170 GHz. Calculations on stress distribution (5 bar overpressure) and a final principle design were done. In contrast to liquid nitrogen cooled windows, such windows always must be operated in an evacuated waveguide in order to avoid freezing and in the case of the torus window a cold trap on the torus side should pump the dust in the waveguide.

Finite element calculations on a large aspect ratio rectangular Brewster window (680 mm x 12 mm) with water edge cooling at 293 K show that Au-doped silicon and PACVD diamond are possible candidates for CW operation around 170 GHz. Diamond is preferable since there is no danger of enhanced losses due to thermal excitation of charge carriers at temperatures higher than 350 K. The window assembly consists of an open-ended corrugated circular HE_{11} waveguide, radiating into a dog-leg configuration consisting of a defocusing and a focusing reflector which generate the highly elongated HE_{11} mode of a corrugated rectangular (200 mm x 12 mm) waveguide that houses the Brewster window. The reflectors are contained in an evacuated box. Behind the window, the back conversion to the circular HE_{11} waveguide is achieved by applying the reflectors in the inversed sequence. The final design is presented. The total losses of the assembly (7.3 %) can be reduced to approximately 3 % by using periodically rippled wall mode converters to generate the 90 % HE_{11} /10 % HE_{12} (in phase) mode mixture for optimum coupling to the free-space Gaussian mode.

Recent measurements on a new PACVD diamond specimen at FZK showed a reduced loss tangent value of $\tan \delta = 2 \cdot 10^{-5}$ so that a conventional circular, water edge-cooled window becomes feasible. Such a window would have a much simpler mechanical structure compared to the medium- and large-aspect ratio rectangular window and would be much easier to handle than a cryo-window.

1. Introduction and Present Status of Experiments

Electron Cyclotron Heating (ECH) is one of the major candidates for H&CD on ITER (170 GHz). ECH is extremely attractive from a reactor engineering point of view, offering compact launch structures, high injected power density, and a simple interface with the shield/blanket. High unit power, in excess of 1 MW, and high-efficiency tubes significantly reduce the system cost by reducing the size of the auxiliary support systems (power supplies, cooling, input power, ...). CW operation is required for some of the anticipated ITER applications: 3s for start-up, 100 s for heating to ignition and 100-1000 s for current drive. In order for the Electron Cyclotron System to perform these functions a window must be developed to serve as both the tritium containment barrier on the torus and as the output window on the tube. The former application is technically more demanding as a torus window must also serve as a high pressure barrier during off-normal events (5 bar overpressure capability), should not use FC-cooling liquid, must not degrade unacceptably under modest neutron and γ irradiation (and X-rays) and in the case of cryo-cooling must be prevented by a cold trap from cryo-pumping. The objective of the present research activity is to develop 170 GHz, 1 MW, CW torus and gyrotron windows for ITER.

From the viewpoint for the realization of 1 MW CW operation, essentially all components of present-day transmission lines and gyrotrons have been developed with the exception of the mm-wave window. At present, edge-cooled (water) single-disk BN and fused quartz windows (EU,RF) as well as surface-cooled (FC-75) double disk sapphire windows (JA, US) are in use in pulsed operation at lower power levels. Cryogenically edge-cooled single disk sapphire windows (EU, JA, RF) [1-10] and distributed windows (US)[11] are under test. The present experimental state-of-the-art is summarized in Table I. As can be seen, no windows for CW applications at the MW power level exist.

Material	Type	Power (kW)	Frequency (GHz)	Pulse Length (s)	Institution
water-free fused silica	single disk inertially cooled	200	60	5.0	UKAEA/Culham
boron nitride	single disk water edge cooled	900	110	2.0	GYCOM (TORIY)
		550	140	3.0	GYCOM (TORIY)
		600	140	2.0	GYCOM (SALUT)
sapphire	single disk LN ₂ edge cooled	485	118	5.0	CEA/CRPP/FZK/ THOMSON
		285*	140	3.0	IAP/INFK
		500	140	0.5	FZK/IAP/IPF/IPP
		370	140	1.3	FZK/IAP/IPF/IPP
sapphire	single disk with Cu anchor LHe edge cooled	410	110	1.0	JAERI/TOSHIBA
sapphire	double disk FC75 face cooled	200	60	CW	CPI
		400	84	10.5	NIFS/CPI
		350	110	10.0	CPI
		350	110	5.0	JAERI/TOSHIBA
		200	140	CW	CPI
		500	170	0.6	JAERI/TOSHIBA
sapphire	distributed water cooled	65**	110	0.3	GA/JAERI/ TOSHIBA
		200*	110	0.7	GA/CPI
diamond	single-disk water edge cooled	300**	110	1	CPI/FOM

Note: * and ** indicates that the power density corresponds to that of a 1 MW (*) and 0.8 MW (**)HE₁₁ mode, respectively

Tab. I: Experimental parameters of high-power millimeter-wave vacuum windows.

2. Material Characterization, Selection and Concepts

In order to define the appropriate concepts for the development of 1 MW, CW millimeter-wave windows one has to compare the thermophysical, mechanical and dielectrical parameters of possible window materials related to the load-failure resistance R' and the power transmission capacity P_T at different temperatures. The features of sapphire, Au-doped Si and PACVD (Plasma Assisted Chemical Vapor Deposition)-Diamond at room temperature and cryo-temperatures are summarized in Tables II and III, where $R' = k \cdot \sigma_B \cdot (1-\nu)/E \cdot \alpha$ and $P_T = R' \rho \cdot c_p / ((1 + \epsilon_r') \cdot \tan\delta)$. The LN₂ edge cooled sapphire window of the 118 GHz TTE gyrotron (0.5 MW, 210 s), that operates close to the allowable lower limits of these two parameters, has $R'=130$ and $P_T=80$. The comparison of R' and P_T for the three window materials clearly shows, that there is no chance to use an edge-cooled, single-disk BN, Si₃N₄ or sapphire window at room temperatures. Experiments at CPI in US and NIFS and JAERI in JA showed, that even a double-disk FC75-face cooled sapphire window has a CW-power limit around 0.3-0.4 MW.

HEMEX sapphire shows identical behaviour of the loss tangent without and after neutron irradiation at 293 K (neutron energy > 0.1 MeV, neutron fluence 10^{21} n/m²) and 77 K ($0.3 \cdot 10^{21}$ n/m²) and there is no measureable in-beam effect (X-ray dose rate up to 0.75 Gy/s) for these neutron-irradiated HEMEX samples. The radiation sensitivity of silicon decreases with increasing electron irradiation dose. For diamond, at the highest X-ray dose rate tested, 3600 Gy/s, no measureable increase in loss is measured. This is most probably due to the high intrinsic defect content of the material. According to Tables II and III the following single-disk window concepts exist. With exception of option 2.1.1 all the other windows have a rim for edge cooling.

2.1 Water-Cooled Windows ($T_0=293$ K)

A water-cooled window has the two very important advantages, that it is employing a cheap, simple and effective coolant and it can be also easily used as torus window:

2.1.1 Distributed Sapphire Window

A novel vacuum window has been developed at General Atomics in US which uses a planar slotted structure of alternating thin sapphire bars with micro-channel water-cooled niobium hexagonal tubes [11]. Analysis indicates that a window 100 mm x 100 mm in area can carry 1 MW in the HE₁₁ mode at 110 GHz and 1 MW with an appropriate HE₁₁/HE₁₂ mode mixture at 170 GHz. The experimental results on such a distributed window are included in Table I. The big disadvantages of this solution are the complicated and expensive mechanical structure, the measured losses of 8 % (at 110 GHz) and the danger of arcing, even in an evacuated waveguide.

2.1.2 PACVD-Diamond Window (Edge Cooled)

As a potential new material for noncryogenically cooled gyrotron windows, diamond is attractive due to its phenomenal tensile strength, modest dielectric constant, relatively low loss and high thermal conductivity. Current PACVD capabilities have allowed for tests with samples of up to 40 mm diameter and 1.1 mm thickness at $f = 145$ GHz [12]. Manufacturers (GEC-Marconi, DeBeers) claim, that they also can produce samples of up to 160 mm diameter. DeBeers company has already manufactured a disk of 105 mm diameter and 2.1 mm thickness.

Tab. II

Thermophysical, Mechanical and Dielectrical Parameters
of Window Materials
related to
Thermal Load -Failure Resistance and Power Transmission Capacity
at Room Temperature (p.c.=poly-crystalline, s.c.=single-crystalline)

Material	BN (CVD) p.c.	Si ₃ N ₄ composite (SN-B)	Sapphire (Al ₂ O ₃) s.c.	Silicon Au-doped s.c.	Diamond (PACVD) p.c.
Thermal Conductivity k [W/mK]	50	59	40	150	1900
Ultimate Bending Strength σ_B [MPa]	80	800	410	3000	600
Poissons Number ν	0.25	0.28	0.22	0.1	0.1
Density ρ [g/cm ³]	2.3	3.4	4.0	2.3	3.5
Specific Heat Capacity c_p [J/g K]	0.8	0.6	0.8	0.7	0.5
Young's Modulus E [GPa]	70	320	385	190	1050
Therm. Expans. Coeff. α [10 ⁻⁶ /K]	3	2.4	5.5	2.5	0.9
Permittivity (145 GHz) ϵ_r'	4.7	7.9	9.4	11.7	5.66
Loss Tangent (145 GHz) $\tan\delta$ [10 ⁻⁵]	115	24	20	0.35	2
Metallizing/Brazing	o.k.	o.k.	o.k.	o.k. (550°C)	o.k. (1000°C) vacuum
Possible Size \varnothing [mm]	145	400	270	127	160
Cost	medium	low	high	low	high
Failure Resistance R' $R' = k\sigma_B(1-\nu)/E\alpha$	14.2	44.5	6.0	852	1086
RF-Power Capacity P _T $P_T = R'\rho c_p/((1+\epsilon_r')\tan\delta)$	0.04	0.45	0.09	318	142
Radiation Sensitivity $n(10^{21}n/m^2)$ γ/X (0.75 Gy/s)			no no	no	no

Tab. III
Thermophysical, Mechanical and Dielectrical Parameters
of Window Materials
related to
Thermal Load -Failure Resistance and Power Transmission Capacity
at LN₂-Temperature - 77 K (LNe-Temperature - 30 K)
(p.c.=poly-crystalline, s.c.=single-crystalline)

Material	Sapphire (Al ₂ O ₃) s.c.	Silicon Au-doped s.c.	Diamond (PACVD) p.c.
Thermal Conductivity k [W/mK]	900 (20000)	1300	10000
Ultimate Bending Strength σ_B [MPa]	410	3000	600
Poissons Number ν	0.22	0.1	0.1
Density ρ [g/cm ³]	4.0	2.3	3.5
Specific Heat Capacity c_p [J/g K]	0.8	0.7	0.5
Young's Modulus E [GPa]	402 (405)	190	1050
Therm. Expans. Coeff. α [10 ⁻⁶ /K]	5.5	2.5	0.9
Permittivity (145 GHz) ϵ_r'	9.3	11.5	5.63
Loss Tangent (145 GHz) $\tan\delta$ [10 ⁻⁵]	0.57 (0.2)	0.35	2
Metallizing/Brazing	o.k.	o.k. (550°C)	o.k. (1000°C) vacuum
Possible Size \varnothing [mm]	270	127	160
Cost	high	low	high
Failure Resistance R' $R' = k\sigma_B (1-\nu)/E\alpha$	130 (2871)	7389	5715
RF-Power Capacity P _T $P_T = R' \rho c_p / ((1+\epsilon_r')\tan\delta)$	71 (4460)	2719	755
Radiation Sensitivity $n(0.3 \cdot 10^{21}n/m^2)$ γ/X (0.75 Gy/s)	no no	no	no

2.1.3 Au-Doped Silicon Window (Edge Cooled)

Another potential window material, an optimized silicon grade, is now also being investigated [13]. For this material in the temperature range between 150 K and 200 K the loss tangent is more than a factor of 100 lower and the thermal conductivity is 3-4 times higher than that of sapphire. Above 70 K the power carrying capability of a silicon window will exceed that of a comparable sapphire window. Calculations show, that a single-disk, water edge-cooled Au-doped silicon window at room temperature is also feasible, if the shape of the window and/or of the power distribution is optimized. Nevertheless one always should not forget, that at temperatures higher than 350 K there is the danger of enhanced losses due to thermal excitation of charge carriers. Therefore, Au-doped silicon is primarily a candidate material for windows operating just below 200 K.

2.1.4 Large-Aspect-Ratio Rectangular Brewster Window

As an alternative to the distributed window concept under development by the US Home Team, the EU Home Team proposed a high-aspect-ratio rectangular waveguide window inclined at the Brewster angle. This concept uses water edge cooling of a single disk made out of silicon or diamond. The window assembly consists of an open-ended corrugated circular HE_{11} waveguide, radiating into a dog-leg configuration consisting of a defocusing and a focusing reflector which generate the highly elongated HE_{11} mode of a corrugated rectangular (200 mm x 12 mm) waveguide that houses the Brewster window. The reflectors are contained in an evacuated box. Behind the window, the back conversion to the circular HE_{11} waveguide is achieved by applying the reflectors in the inversed sequence (FZK-ITER TASK T25, Subtask 3, this report) [1].

2.2 CHF_3 or CF_3CL Edge-Cooled Windows ($T_0 \leq 200$ K)

If one allows a gyrotron window to function with a simple cryo-coolant like CHF_3 or CF_3CL , the temperature range around 180 K is optimum for a Au-doped silicon window since under these conditions this material has $\tan\delta = 3 \cdot 10^{-6}$ and $k = 250$ W/mK, so that an edge cooled single-disk version would be feasible [13].

2.3 Liquid Nitrogen Edge-Cooled Windows ($T_0=77$ K)

The microwave energy absorbed in the window is removed by nucleate boiling liquid nitrogen at atmospheric pressure (77 K) [2-4].

2.3.1 Sapphire Window

The theoretical power limits for CW transmission of a single disk, LN_2 edge-cooled circular sapphire window (I.D. = 88.9 mm) are given in Table IV. The overpressure capability is only approximately 2 bar. The loss tangent of sapphire scales with the frequency f .

	140 GHz	170 GHz	220 GHz
Gaussian Profile (G)	0.5 MW	0.4 MW	0.3 MW
Flattened Profile (F)	0.7 MW	0.6 MW	0.45 MW
Annular Profile (A)	1.0 MW	0.85 MW	0.65 MW

Table IV: Maximum power transmittance of a single disk, LN₂ edge-cooled, circular sapphire window with resonant thickness ($5\lambda/2$ at 140 GHz, $6\lambda/2$ at 170 GHz, $8\lambda/2$ at 220 GHz) for different power distributions.

The present experimental status of circular LN₂-edge cooled single disk sapphire windows is also summarized in Table I. A performance of 0.49 MW for 5s was achieved with the European 118 GHz gyrotron manufactured by TTE [9].

FZK (FZK-ITER Task T25, Subtask 1, this report) and IAP have operated the windows at atmospheric pressure. Owing to specific cold N₂-gas flushing systems the windows could be operated with minor freezing and rf-arcing problems during a whole working day. After 6 hours operation of the FZK experiment a thin layer of ice has been observed on the surface of the window disk. At the position of the beam center, this layer could be removed by means of a short gyrotron pulse, showing a possibility to clean the window.

FZK experiments using a copper disk heater have shown, that by atmospheric evaporative cooling in liquid nitrogen, up to 1300 W can be safely removed at the edge of the window. This means that it is not the heat removal at the edge which limits the power transmittance of the window, but the radial removal of the heat absorbed in the window itself which already at 200 to 300 W causes so-called thermal runaway. This leads to the concept of a medium aspect ratio elongated window. The use of an elliptical millimeter-wave beam with a rectangular, racetrack or elliptical window increases the power and overpressure capabilities (FZK-ITER Task T25, Subtask 2, this report) [1].

2.3.2 Au-doped Silicon Window

Table III shows the excellent parameters of Au-doped silicon at $T=77$ K. Such a window clearly has the potential of 2 MW, CW operation in the millimeter range (Gaussian power distribution). The favourable frequency scaling of $\tan\delta$ with f^{-1} allows also to go to higher frequencies than 170 GHz. Since $\tan\delta$, in the temperature range from 77 to 200 K, is nearly constant, there is no danger of runaway as for sapphire. The saturation of absorption with increasing power in silicon in strong electromagnetic fields in the mm-wavelength range could lead to an absorption reduction by a factor of 1.5 to 2 compared to linear scaling with power [14].

2.4 Cryogenic Sapphire Window at $T_0=20-30$ K

Lowering the temperature of a sapphire window to $T = 20-30$ K results in a strong reduction of $\tan\delta$ and permits operation in the range of maximum thermal conductivity. The power transmittance capability increases at least by a factor of 5.6, allowing even 2 MW windows at 170 GHz in a to be operated with a Gaussian beam. However, in contrast to liquid nitrogen cooled windows, such windows always must be operated in an evacuated waveguide in order to avoid freezing.

For heat removal one can use forced He-gas flow or, more simply, a liquid helium cooled thermal copper anchor around the window disk. Another possibility is the use of nucleate boiling liquid neon (neon bath) at atmospheric pressure (27.15 K). Neon could be simply liquefied by making use of an available flow of cold He gas (FZK-ITER Task T 25, Subtask 4 this report).

3. Potential Options

Table V summarizes potential options for 1 MW, CW, 170 GHz operation. Options ① to ③ being water cooled, are preferred for their simplicity, in particular for use as a torus window.

	Material	Type	RF-Profile	Cross-Section	Cooling
①	Sapphire/Metal	distributed	flattened Gaussian	rectangular (100 mm x 100 mm)	internally water cooled (300 K) $\tan\delta = 2.5 \cdot 10^{-4}$, $k = 40$ W/mK
②	Diamond	single-disk	Gaussian	circular ($\varnothing = 80$ mm)	water edge cooled (300 K) $\tan\delta = 2 \cdot 10^{-5}$, $k = 1900$ W/mK
③	Diamond	single-disk Brewster	Gaussian	rectangular (680 mm x 12 mm)	water edge cooled (300 K) $\tan\delta = 2 \cdot 10^{-5}$, $k = 1900$ W/mK
④	Silicon Au-doped	single-disk	flattened Gaussian	circular ($\varnothing = 80$ mm)	edge cooled (200 K), cryo-cooler (CHF_3 , CF_3Cl) $\tan\delta = 3 \cdot 10^{-6}$, $k = 250$ W/mK
⑤	Silicon Au-doped	single-disk	Gaussian	circular ($\varnothing = 80$ mm)	LN_2 edge cooled (77 K) $\tan\delta = 4 \cdot 10^{-6}$, $k = 1500$ W/mK
⑥	Sapphire	single disk	flattened Gaussian	rectangular (285 mm x 35 mm)	LN_2 edge cooled (77 K) $\tan\delta = 6.7 \cdot 10^{-6}$, $k = 1000$ W/mK
⑦	Sapphire	single disk	Gaussian	circular ($\varnothing = 80$ mm)	LNe or LHe edge cooled (27 K) $\tan\delta = 1.9 \cdot 10^{-6}$, $k = 2000$ W/mK

Note that the power capability of options ②, ⑤ and ⑦ is even 2 MW.

Tab. V: Options for 1 MW, CW, 170 GHz ECH windows.

4. Performance Targets and Development Strategy

Distributed Window ①

R&D is being performed by the US (General Atomics and CPI), collaborating with Japan for the high power test.

PACVD-Diamond Windows ②③

The use of PACVD diamond as a window material for microwave tubes is investigated within a three years Brite-EURAM III Programm (1996-1998) with the following partners: GEC Marconi, Thomson TTE, Aixtron, Thomson CSF, CIEMAT, Madrid, FZK Karlsruhe, Univ. Saarbrücken, CNRS, Laser Ecosse, CEA Cadarache.

Neutron irradiation tests at a neutron fluence of 10^{21} n/m² will be performed by FZK in 1996 under the ITER Task T246.

Window option ② is preferable to ① and ③ since its mechanical structure is much simpler.

Au-Doped Silicon Windows ④⑤

The material preparation and characterization has been done in collaboration between EU (FZK) and RF (IAP). Neutron irradiation test will be performed in 1996 by FZK.

Window option ⑤ is preferable to ④ since it has better power transmission capability, allows for a simple Gaussian beam and employs LN_2 cooling which can be used at the torus (together with a cold trap) and also can be operated at atmospheric pressure.

***Elongated LN₂-Cooled Sapphire Window* ⑥**

An assessment and design of a medium aspect ratio elongated liquid nitrogen edge cooled single disk sapphire window for 170 GHz, 1 MW, CW operation has been performed by FZK as ITER TASK T25- Subtask 2 [1].

The manufacturing feasibility of such large-area racetrack-shaped sapphire windows was proven by Kyocera Corporation in Japan in collaboration with NIFS Nagoya. They have succeeded in the production of a large-size C-cut single crystalline sapphire disk by the so-called edge-defined-film-fed growth method, minimizing distortions of the disk under metallizing and brazing processes. They have manufactured a racetrack-shaped window with an effective area of 240 mm x 65 mm [10].

Such a window should be used if there are problems with window options ②, ⑤ and ⑦.

***Circular LNe-Cooled Sapphire Window* ⑦**

In 1996, FZK Karlsruhe in collaboration with TTE Velizy will fabricate a liquid neon edge cooled single disk sapphire window for 118 GHz, 0.5 MW, > 10s operation and will test it at CEA Cadarache using the European 118 GHz, 0.5 MW, 210 s gyrotron (FZK-ITER Task T245/6). In 1997 a 170 GHz, >0.5 MW, >10 s window could then be tested in collaboration with Japan as part of the ITER activity.

For 0.5 MW, 118 GHz, 210 s operation the power absorbed by the window disk will be around 29 W and the maximum and minimum temperatures are calculated to be $T_{\max} = 30$ K and $T_{\min} = 27$ K, respectively. The closed-cycle neon refrigeration system "Philips Cryogenerator PH 110" (refrigeration capacity: 150 W) available at FZK Karlsruhe could be used for first experimental tests on such a window system. An approximately 4 m long LNe-transmission line to the window cryostat was purchased from cryo-industries and is now available at FZK. Test runs of the cryogenerator were successful.

The window test will be performed at CEA Cadarache employing an improved version of the TTE 118 GHz gyrotron window assembly [9] in an evacuated waveguide run. Special care has to be taken in order to minimize the static liquid neon consumption (most critical issue). The commissioning of the window assembly is under way.

The present ITER ECH Window Development Task T25 (EU) consists of the following subtasks:

- Subtask 1: High power experiment (140 GHz, 0.5 MW, 1s) for determination of the power absorbed in a liquid nitrogen edge cooled single disk sapphire circular window (high power window calorimeter). Validation of the parameters of sapphire.
- Subtask 2: Assessment and design of a medium aspect ratio rectangular liquid nitrogen edge cooled single disk sapphire window for 170 GHz, 1 MW, CW operation.
- Subtask 3: Assessment and design of a non-cryogenic, large-aspect-ratio rectangular, water-cooled single disk torus window system.
- Subtask 4: Optimization and design of a liquid neon edge cooled single disk sapphire window for 1 MW, CW operation.

5. Subtask 1: High power experiment (140 GHz, 0.5 MW, 1s) for determination of the power absorbed in a liquid nitrogen edge cooled single disk sapphire circular window (high power window calorimeter). Validation of the parameters of sapphire.

Summary

A series of experiments were performed in collaboration of FZK, IPP Garching and IPF Stuttgart with an optimized liquid nitrogen cooled sapphire (HEMEX) window calorimeter (disk diameter $D=140$ mm, disk thickness $d=3.51$ mm) operated at atmospheric pressure in the pulsed beam of a Russian GYCOM/SALUT 140 GHz gyrotron (≤ 0.5 MW, ≤ 1.3 s). The test facility acts as a calorimeter such that the energy absorbed during a shot is obtained from measurements of the temperature raise. Such experiments also allow to study problems related to high power transmission through an atmosphere at temperatures between 80 K and 300 K (e.g. fog formation in the waveguide section and freezing on the window disk). The window is embedded in a thermally insulated Cu box cooled by a LN_2 flow. Mounted on a pneumatically driven slide, the window is moved to "in-beam position" during the rf pulse. After the gyrotron shot it is removed into the "calorimeter position" where the increase of temperature is detected by eight thin film sensors pressed by magnetic actuators to different parts of the window disk. Owing to the optimized N_2 -gas flushing system the window calorimeter could be operated with minor freezing and rf-arcing problems during a whole working day. After 6 hours of the mentioned operation a very thin layer of ice has been observed on the surface of the window disk. At the position of the beam center this layer could be removed by means of a short gyrotron pulse, showing a possibility to clean the window.

The window calorimeter has proven to operate satisfactorily during a series of approximately 50 gyrotron shots (140 GHz, 0.37 -0.5 MW, 1.3 s-0.5 s, Gaussian power distribution with a beam waist of $w_0 = 35$ mm). Within the experimental uncertainties the measured $\tan\delta$ -values of $(8\pm 4) \cdot 10^{-6}$ in the temperature range between 87 and 95 K are in good agreement with cold test measurements (FZK, Heidinger, 145 GHz) on a HEMEX-sapphire specimen (Crystal Systems), taking into account the linear frequency scaling.

5.1. Experimental Method

The test facility acts as a calorimeter such that the energy absorbed during a shot is obtained from measurements of the increase of the average temperature of the window disk. If power and duration of the gyrotron pulse are known, the temperature averaged loss tangent of the window material can be obtained following eqs. (1) to (3):

absorbed energy at resonance thickness ($d = n \cdot \frac{\lambda}{2}$):

$$Q_{\text{abs}} = P_{\text{gyr}} \cdot \Delta t \frac{\pi f d \tan \delta (1 + \epsilon_r')}{c_o} \quad (1)$$

average temperature raise:

$$\Delta T = Q_{\text{abs}} / \left(\rho \frac{\pi}{4} D^2 d \cdot c_p \right) \quad (2)$$

temperature averaged loss tangent:

$$\tan \delta = \frac{c_o \rho D^2 c_p}{4f (1 + \epsilon_r')} \cdot \frac{\Delta T}{P_{\text{gyr}} \Delta t} \quad (3)$$

P_{gyr}	=	gyrotron power
Δt	=	pulse duration
f	=	frequency
c_o	=	velocity of light in air
ϵ_r'	=	relative permittivity
ρ	=	specific density
D	=	disk diameter
d	=	disk thickness
c_p	=	specific heat capacity

The HEMEX (Crystal Systems)-sapphire disk of the window calorimeter has a diameter $D = 140$ mm and a thickness $d = 3.51$ mm. An example of a transient calculation using the finite element code ABAQUS shows that for a 140 GHz, 0.5 MW, 1 s gyrotron pulse the central disk temperature rises from around 80 K to almost 160 K (here, pessimistic values of $\tan \delta$ have been used) and, subsequently, the steady-state condition is practically reached within 2 seconds. The steady-state temperature exceeds the initial temperature by the certain amount ΔT that depends on the absorbed energy (Fig. 1). A comparison of computed and measured ΔT values yields in the measured values of $\tan \delta$.

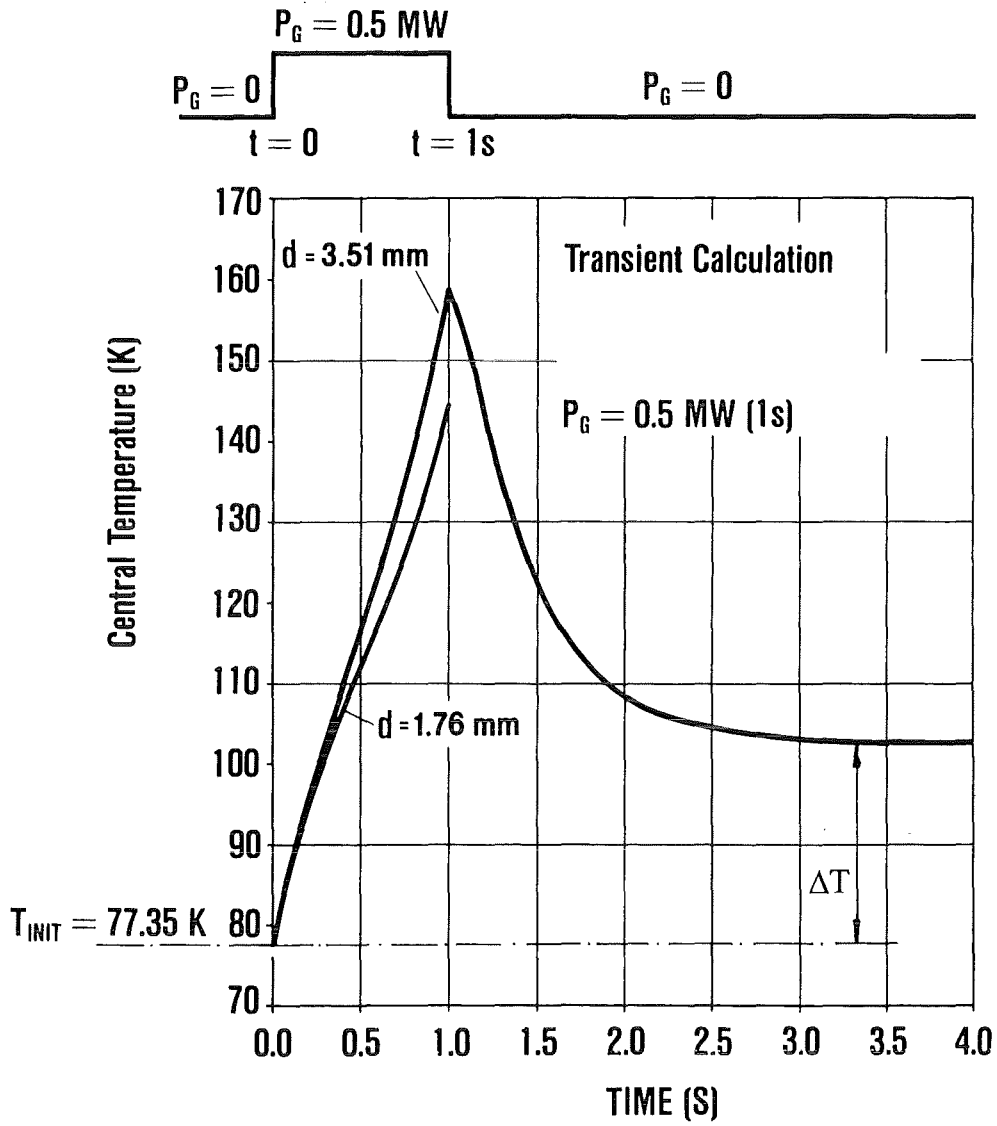


Fig. 1: Computed window center temperature during and after a gyrotron pulse.

5.2. Experimental Arrangement

The window calorimeter consists of a box-shaped central part and the two beam ducts through which the mm-wave beam enters the box and leaves it, respectively (Fig.2). The window is embedded in a thermally well insulated Cu-box cooled by a LN₂ flow. Mounted on a pneumatically driven slide, the sapphire disk can be moved to the in-beam position during the rf pulse. After the gyrotron shot it is immediately removed into the "calorimeter position" where the increase of temperature is measured by means of eight thin-film thermocouples pressed by magnetic actuators to different positions of the window disk. The whole procedure takes less than 0.5 s.

On both sides of the window disk with its displacement mechanism, gate valves are installed with similar sliding mechanisms by which axial heat transfer by convection through the beam ducts towards the window should be avoided. Shortly before and during the mm-wave pulse these shutters are opened. An electronic sequence control is used to control the timing of the various movements (window disk, shutters, lifting magnets for the temperature sensors) and of the gyrotron pulse. Owing to the optimized N₂-gas flushing system at the end of both beam ducts, the window calorimeter could be operated with minor freezing and rf-arcing problems during a whole working day. After 6 hours of operation a very thin layer of ice has been observed on the surface of the sapphire disk. At the position of the beam center this layer could be removed by means of a short gyrotron pulse, showing a possibility to clean the window. Crucial for the successful operation was a soft, diffuse flow of the LN₂ gas instead of well directed gas streams. Fig. 3 shows the complete experimental set-up of the gyrotron, the beam matching optics, the cryo-window calorimeter and the fire-brick load. The rf power was measured using a calorimetric load at the position of the third mirror.

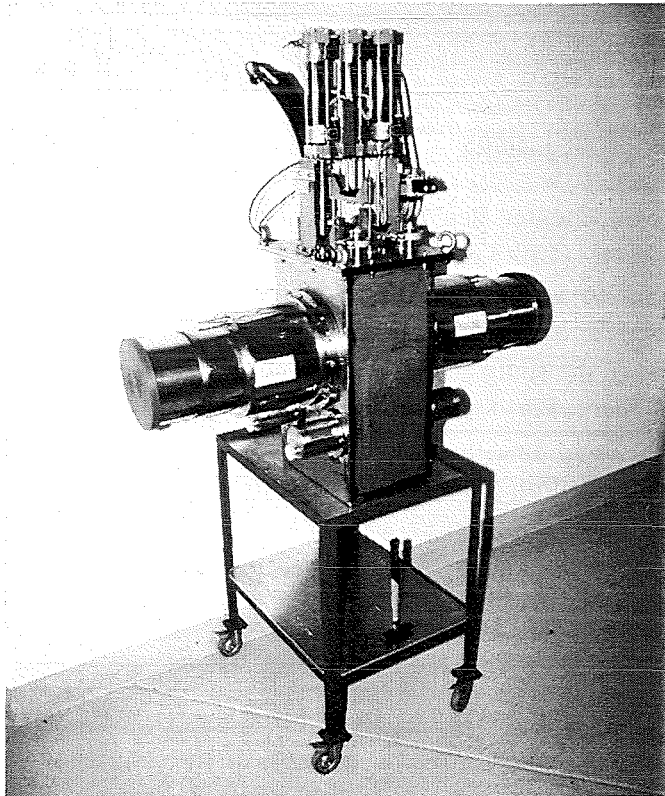
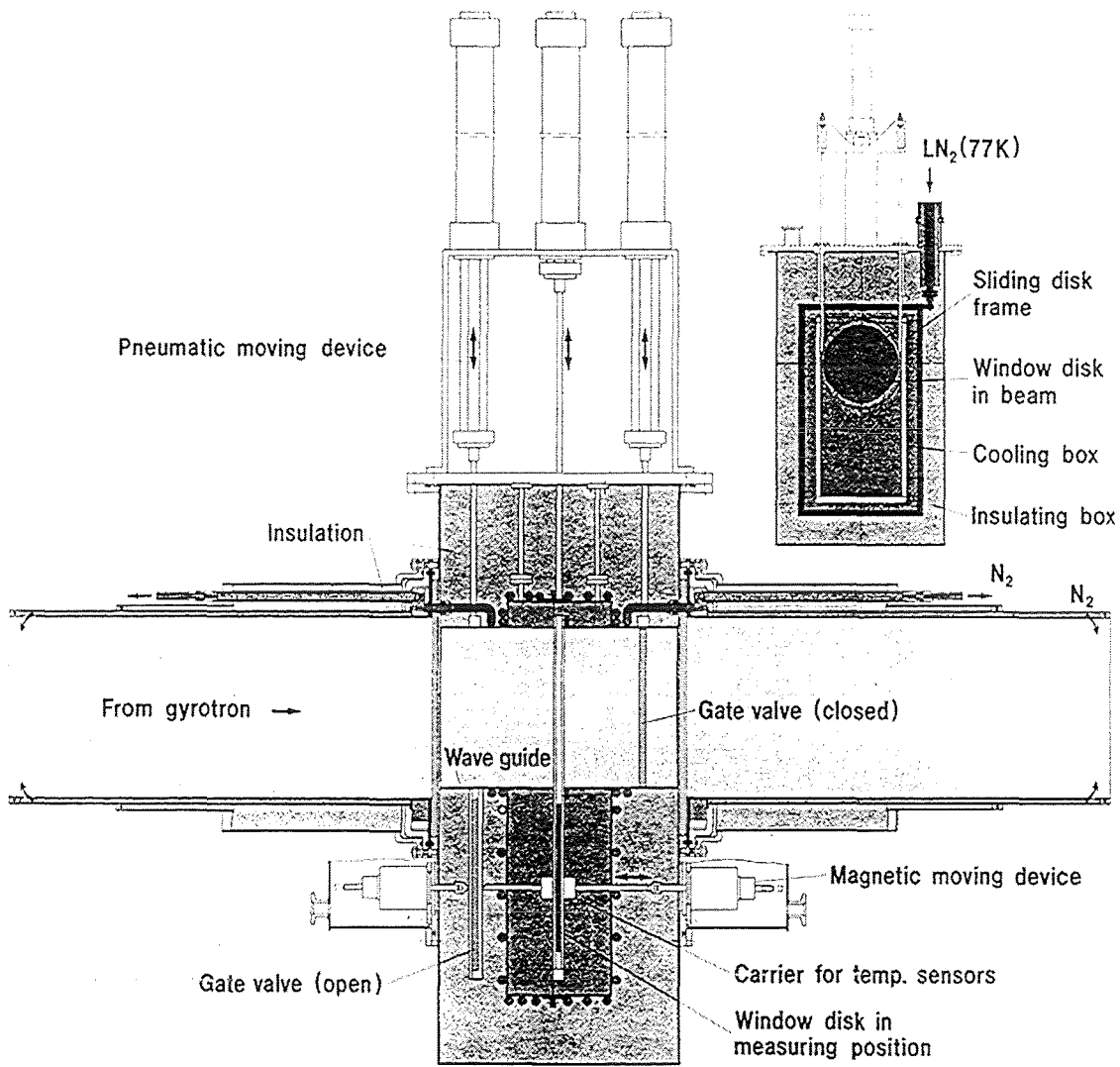


Fig. 2: Schematic and Photograph of the window calorimeter assembly.

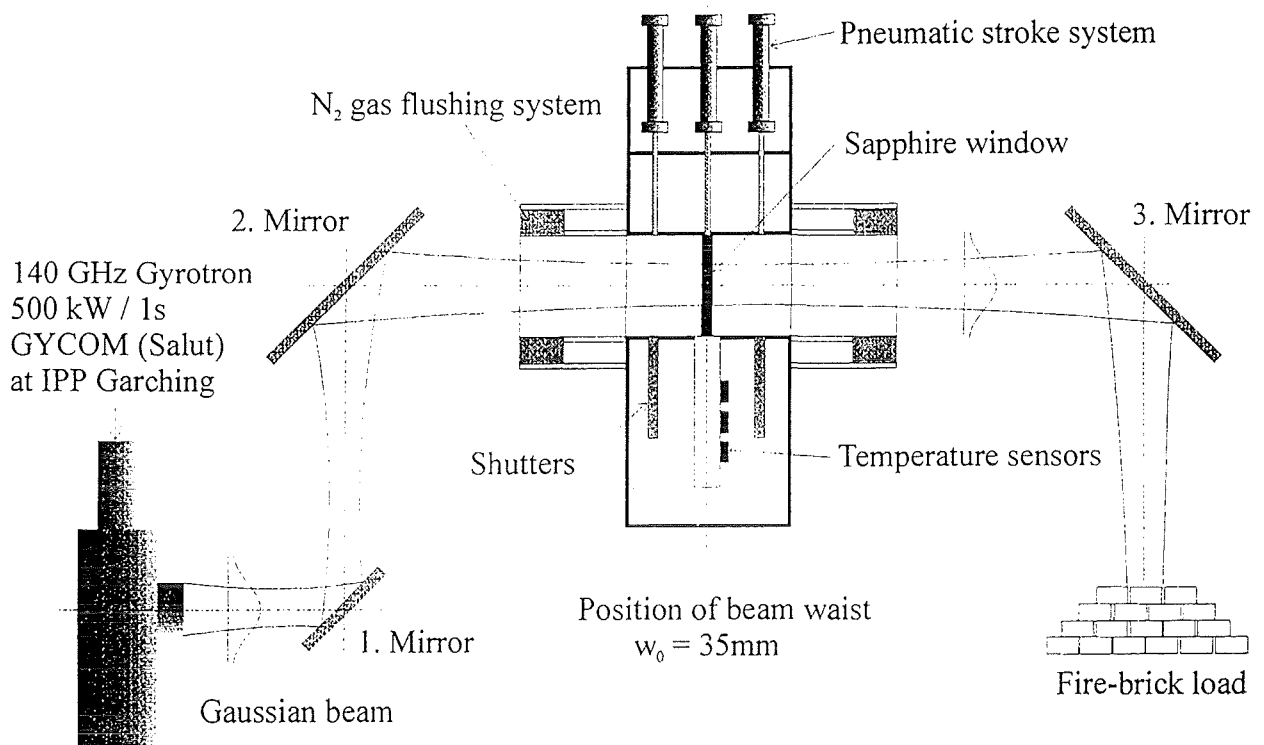


Fig. 3: Setup of the cryo-calorimeter experiment.

5.3 Experimental Results and Conclusions

The cryo-sapphire-window calorimeter has proven to operate satisfactorily during a series of approximately 50 gyrotron shots (140 GHz, 0.73 - 0.5 MW, 1.3 s - 0.5 s, Gaussian power distribution with a beam waist of $w_0 = 35\text{ mm}$). In Fig. 4 the comparison of experimental and theoretical window temperature for a 0.45 MW pulse of 250 ms duration is plotted. The theoretical curve was computed by means of the finite element code using the low power $\tan\delta$ values measured by [15]. The agreement is excellent. Fig. 5 shows the temperature dependence of the loss tangent of various sapphire grades at 145 GHz measured at low power together with the present high power experimental values at 140 GHz. Within the experimental uncertainties the measured $\tan\delta$ values of $(8\pm 4) \cdot 10^{-6}$ in the temperature range between 87 and 95 K are in good agreement with the cold test measurements, taking into account the linear frequency scaling. The dashed curve in Fig. 5 gives the theoretical results of the 2-phonon-model [15,16].

The results show the unusually high $\tan\delta$ -values derived from high power experiments on a cryo-sapphire-window at JAERI in Japan (Fig. 6) [5,6] are not true for HEMEX sapphire. The reasons for this disagreement might be an additional parasitic heating of the JAERI window arrangement by high order modes reflected from the load or a low quality sapphire grade.

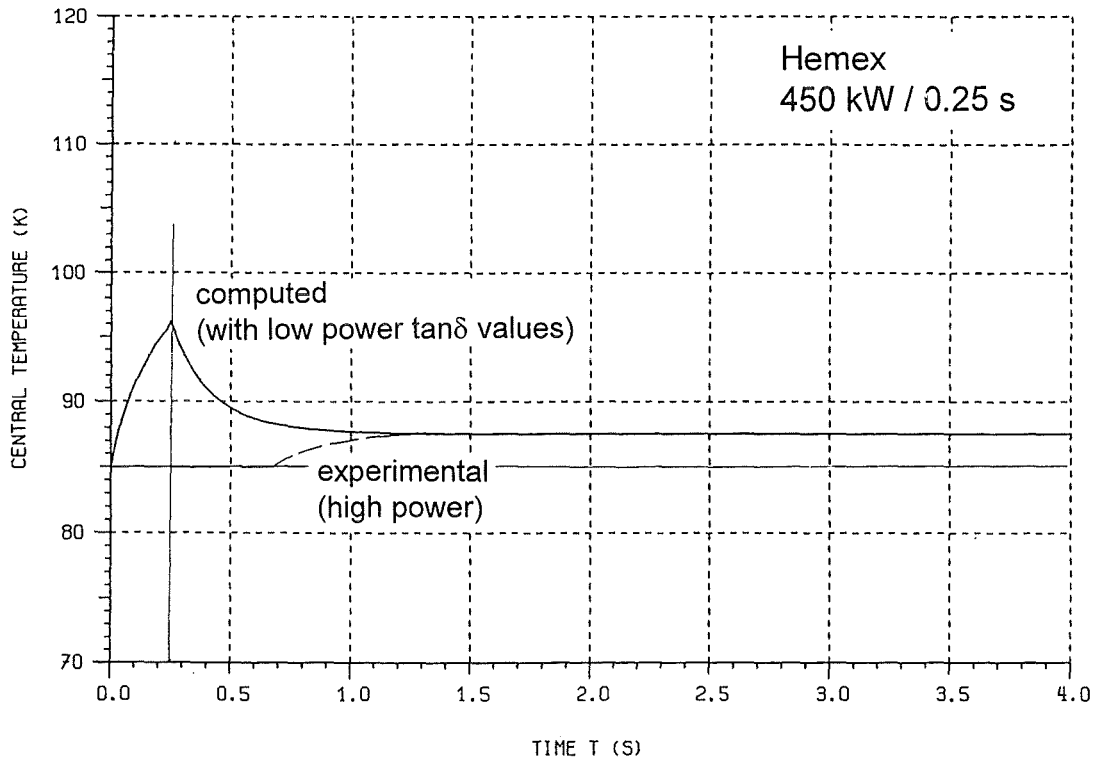


Fig. 4: Comparison of experimental and theoretical window temperature.

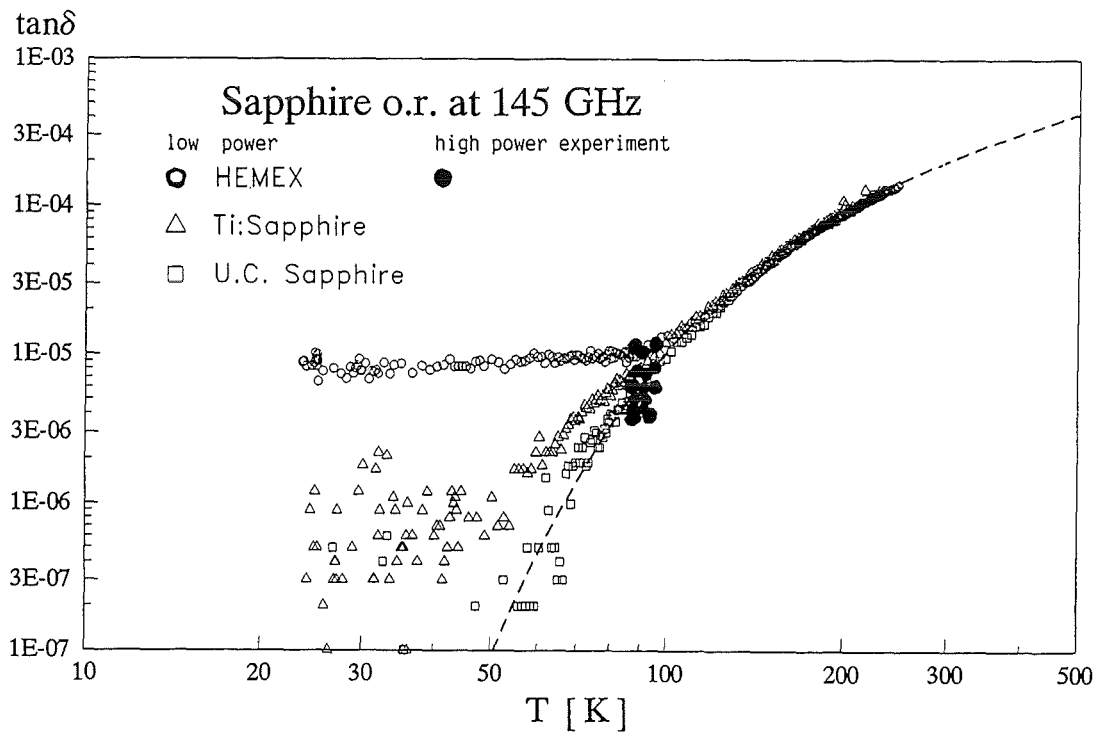
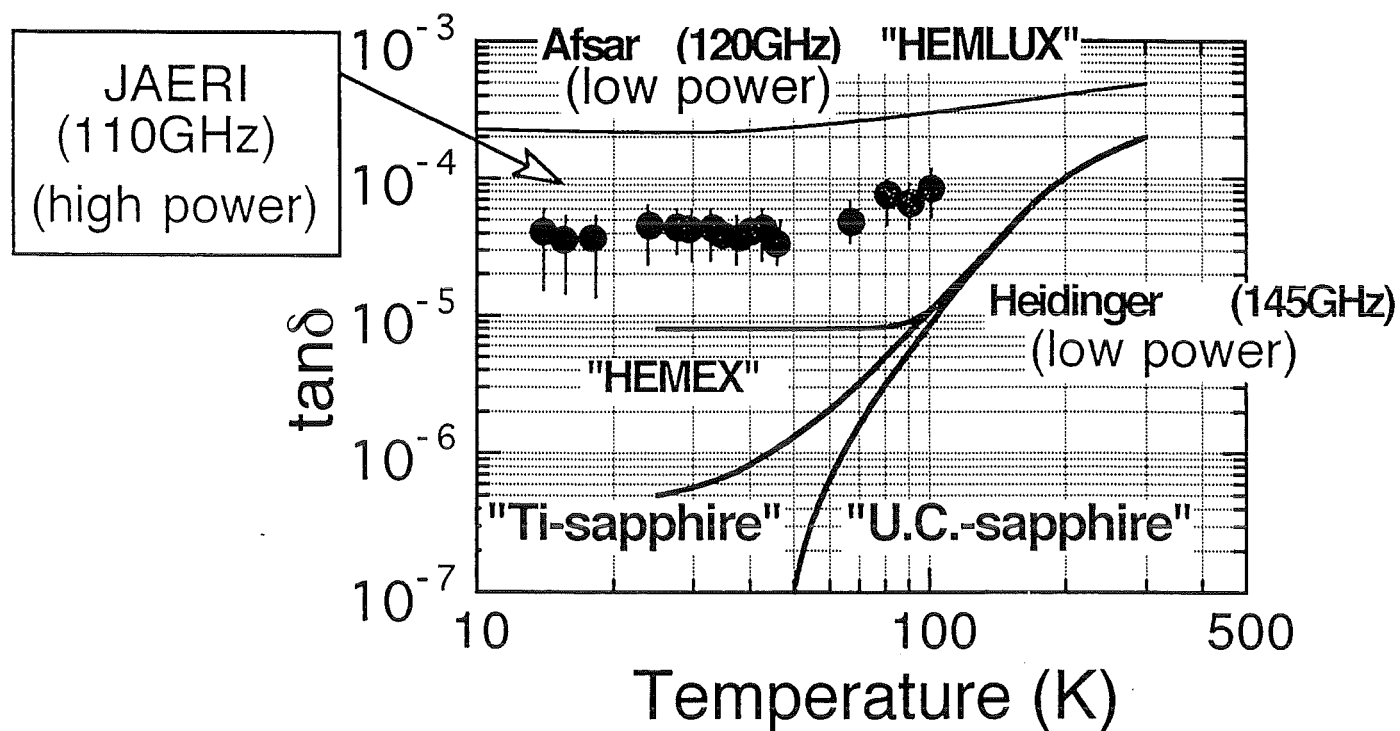


Fig. 5: Dielectric loss of various sapphire grades at cryogenic temperatures.



$\tan\delta$ of our sapphire is $\sim 4 \times 10^{-5}$ at $< 50\text{K}$

(Ref. : Afsar, et al, Int.Journal of ir & mm wave, Vol.15(1994)/ITER Report by EU team(1994))

Fig.6: Results of the high-power cryo-sapphire-window experiments at JAERI.

6. Subtask 2: Assessment and design of a medium aspect ratio rectangular liquid nitrogen edge cooled single disk sapphire window for 170 GHz, 1 MW, CW operation.

Summary

Detailed calculations and design studies on the temperature and thermomechanical behavior for a realistic window assembly employing a racetrack or elliptical geometry and a flexible brazing collar have been performed using the finite element code ABAQUS supported by the pre-processor code FEMGEN for preparation of the discretization mesh.

The use of elliptical windows with a flattened elliptical beam with an aspect ratio of 8:1 (window aperture $a = 252$ mm \times $b = 32$ mm, disk thickness $d = 1.74$ mm) or of a ring-shaped elliptical beam with an aspect ratio of 3:1 (window aperture 156 mm \times 52 mm, disk thickness $d = 1.74$ mm) allows a power transmission capability of 1 MW at 170 GHz without thermal runaway. The absorbed power at 1 MW beam power is 340 W and 285 W, respectively.

Calculations on stress distribution and overpressure capabilities have shown that all stresses are well below the admissible limit (at 5 bar pressure difference) since the measured bending tensile strength of HEMEX sapphire is around 500 MPa and the compressive strength is approximately 2800 MPa.

The manufacturing feasibility of such large-area racetrack-shaped sapphire windows was proven by Kyocera Corporation in Japan in collaboration with NIFS Nagoya. They have succeeded in the production of a large-size C-cut single crystalline sapphire disk by the so-called edge-defined-film-fed growth method and in minimizing distortions of the disk under metallizing and brazing processes. By this process a racetrack-shaped window with an effective area of 240 mm \times 65 mm has been manufactured [10].

6.1. Concept of Elongated Sapphire Window

Design calculations have been performed using the finite element code ABAQUS supported by the pre-processor code FEMGEN for preparation of the discretization mesh. This computational tool allows the temperature and stress distribution in the window disk to be determined in a reliable manner. The original FZK cryowindow design was based on a single circular disk of 140 mm diameter and 1.74 mm thickness ($6 \lambda/2$) in a short cylindrical aperture structure of about 90 mm diameter (Fig. 7). The microwave energy absorbed in the window is removed by nucleate boiling liquid nitrogen at atmospheric pressure (77 K) in a rim around the edge of the disk. Three different power distributions in the window have been chosen for the calculations: (1) fundamental Gaussian (G) wave beam profile (or HE_{11} mode distribution); (2) flattened (F) Gaussian beam profile and (3) ring-shaped, annular (A) beam profile (Fig. 8). Using a power absorption factor $\tan\delta = 3.15 \cdot 10^{-12} \cdot f(\text{GHz})/140 \cdot T^{3.3}$ (K) (R. Heidinger, FZK) together with the best values of thermal conductivity (highest purity) given by Touloukian the maximum calculated CW transmittance of the circular window is: (G) 0.4 MW; (F) 0.6 MW; (A) 0.85 MW. FZK experiments have shown, that by atmospheric evaporative cooling in liquid nitrogen, up to 1300 W can be safely removed at the edge of the window. This means that it is not the heat removal at the edge which limits the power transmittance, but the radial removal of the heat absorbed in the window itself which already at 200 to 300 W causes thermal runaway. This directly leads to the concept of a medium aspect ratio elongated window. The advantage of such a large-area elongated window is that the maximum mechanical stress can be weakened, in comparison to that of a circular disk window with the same surface area and that the heat conduction is improved.

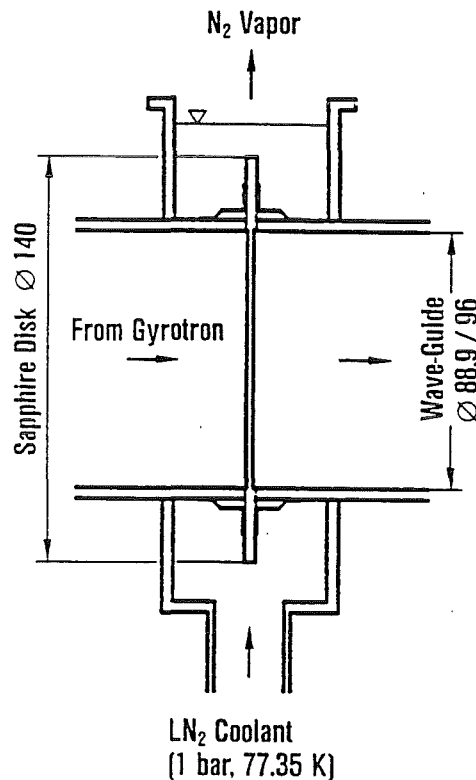


Fig. 7: Principle of the window concept.

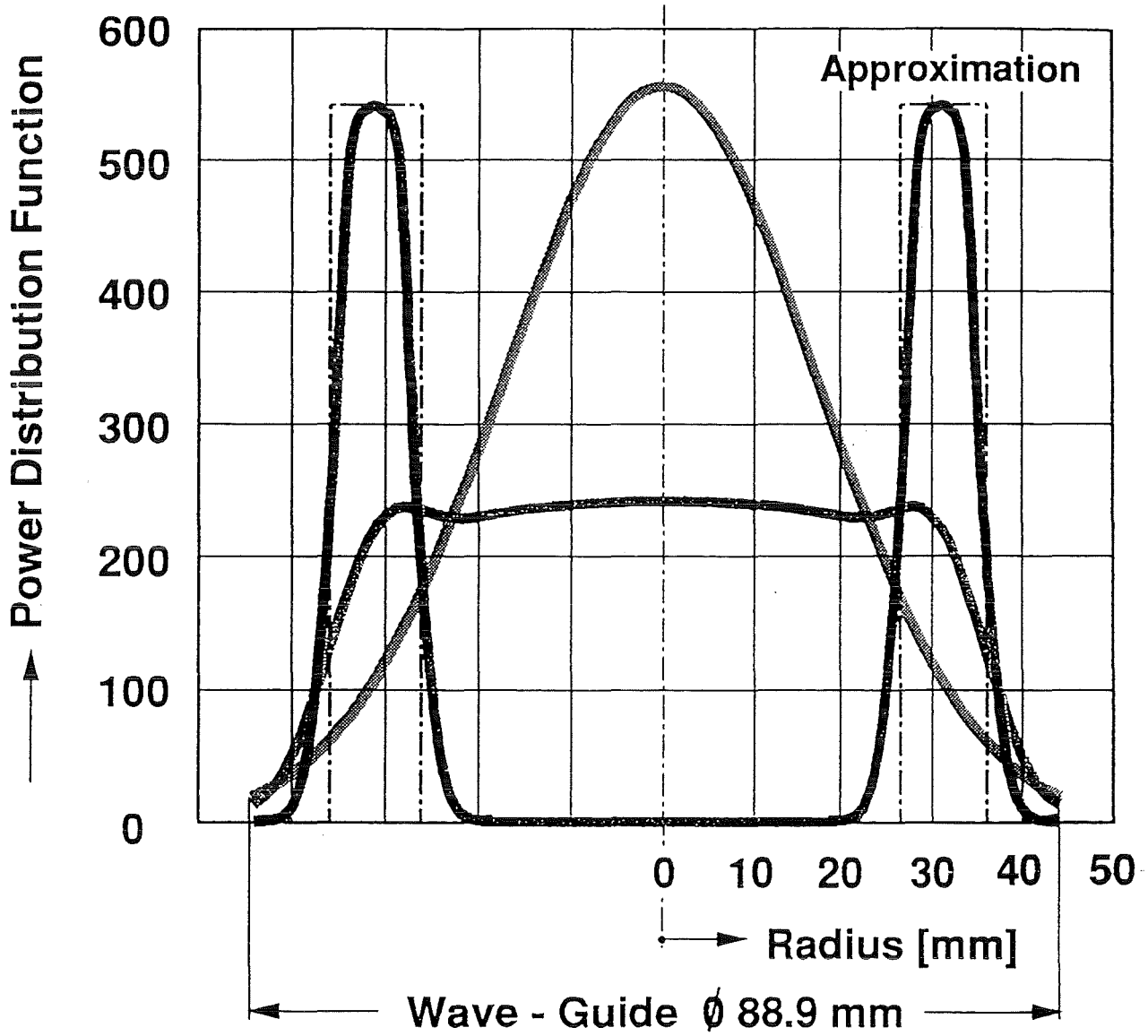


Fig. 8: Different power density distributions of the mm-wave beam.

6.2. Calculation of Power Capabilities

Table VI summarizes the computational results on the power transmittance capabilities of rectangular windows at 170 GHz, CW:

Aperture Size	Aspect Ratio	Elliptical Beam Profile	Max. Power Transmission	Absorbed Power
180 mm x 45 mm	4 : 1	G	0.58 MW	173 W
252 mm x 32 mm	8 : 1	G	0.77 MW	254 W
270 mm x 30 mm	9 : 1	G	0.84 MW	227 W
180 mm x 45 mm	4 : 1	F	0.77 MW	235 W
252 mm x 32 mm	8 : 1	F	1.06 MW	376 W
270 mm x 30 mm	9 : 1	F	1.18 MW	354 W
126 mm x 63 mm	2 : 1	A	0.88 MW	278 W
156 mm x 52 mm	3 : 1	A	1.00 MW	316 W
180 mm x 45 mm	4 : 1	A	1.20 MW	352 W

Tab. VI: Power transmission capability of medium aspect-ratio rectangular sapphire windows with LN₂ edge cooling.

The use of a flattened elliptical beam (F) with an aspect ratio of 8:1 (window aperture 252 mm x 32 mm) or of a ring-shaped elliptical beam (A) with an aspect ratio of 3:1 (window aperture: 156 mm x 52 mm) allows a power transmission capability of 1 MW at 170 GHz. Much higher aspect ratios are required for elliptical Gaussian beams (G). The transmission capability of an elliptical window is 10 % higher than that of a rectangular window with the same aspect ratio.

6.3. Analytical Calculations on Stress Distributions

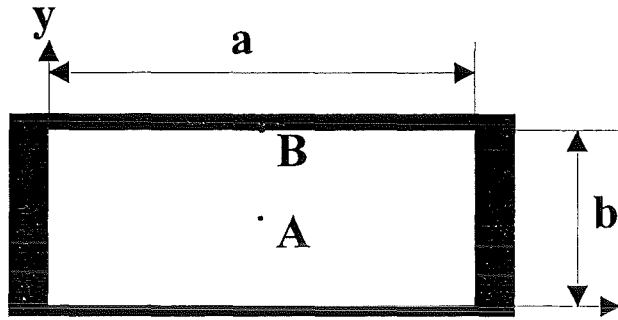
Calculations on stress distribution and overpressure capabilities under simplified assumptions with respect to the brazing collar (all edged pinned) have been performed for a window disk thickness of $d = 1.74$ mm.

The Tables VII and VIII summarize the analytical formulas for the calculation of various distributions for rectangular and elliptical windows. The circular window exhibits at a full pressure difference of $\Delta p = 5$ bar a maximum tensile stress of 160 MPa and compressive stress of 250 MPa, values that are a factor of two below the admissible measured limits of 500 MPa and 2800 MPa, respectively. Elongated windows experience lower stresses than circular windows. The stresses decrease with increasing aspect ratio provided that the area of the window remains constant. As expected, the elliptical shape offers a somewhat higher overpressure capability.

Rectangular window case:

Dimension values are:

a : b	a (mm)	b (mm)
1 : 1	89	89
2 : 1	126	63
3 : 1	156	52
4 : 1	180	45
9 : 1	270	30
57 : 1	672	12



d = 1.74 mm

Stress formulas:

Center(A):

$$\sigma_x = A_x p \frac{b^2}{d^2}$$

$$\sigma_y = A_y p \frac{b^2}{d^2}$$

$$\sigma_{\max} = D_1 p \frac{b^2}{d^2}$$

Edge(B):

$$\sigma_x = B_x p \frac{b^2}{d^2}$$

$$\sigma_y = B_y p \frac{b^2}{d^2}$$

$$\sigma_{\max} = D_2 p \frac{b^2}{d^2}$$

Coefficients:

a : b	A _x	A _y	D ₁	B _x	B _y	D ₂
1 : 1	0,1350	0,1350	0,1386	0,0925	0,3125	0,3078
2 : 1	0,2675	0,1050	0,2472	0,1500	0,5000	0,4974
3 : 1	0,2925	0,1125	0,2500	0,1550	0,5200	0,5000
4 : 1	0,2975	0,1125	0,2500	0,1550	0,5275	0,5000
9 : 1	0,3025	0,1100	0,2500	0,1575	0,5525	0,5000
57 : 1	0,3000	0,1100	0,2500	0,1575	0,5525	0,5000

If we take care of the given window size, the formulas become:

Center(A):

$$\sigma_x = \alpha_x p$$

$$\sigma_y = \alpha_y p$$

$$\sigma_{\max} = \delta_1 p$$

Edge(B):

$$\sigma_x = \beta_x p$$

$$\sigma_y = \beta_y p$$

$$\sigma_{\max} = \delta_2 p$$

and coefficients are:

a : b	α _x	α _y	δ ₁	β _x	β _y	δ ₂
1 : 1	353	353	363	242	817	805
2 : 1	350	138	324	197	656	652
3 : 1	261	100	223	138	464	447
4 : 1	199	75	167	103	352	334
9 : 1	89	32	74	47	157	148
57 : 1	14	5	12	7	26	24

Example of calculation:

a : b = 2 : 1

Δp = 5 bars

σ_x = α_x p = 350 * 5 = 1750 bars so 175 MPa

a : b = 3 : 1

Δp = 5 bars

σ_x = α_x p = 261 * 5 = 1305 bars so 130.5 MPa

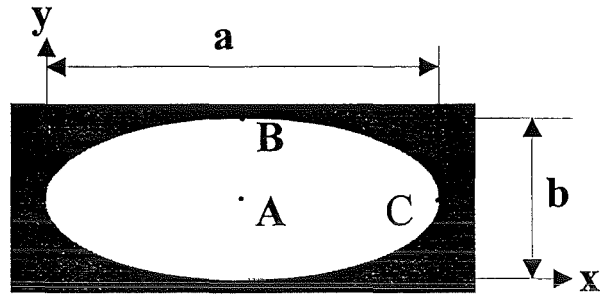
All coefficients are positive in order to not confuse between Tensile Strength and Compressive Strength when you want to check the window limits. (Compressive Strength >> Tensile Strength)

Table VII: Mechanical stress in rectangular windows due to a pressure difference Δp.

Elliptical window case :

Dimension values are:

a : b	a (mm)	b (mm)
1 : 1	89	89
2 : 1	126	63
3 : 1	156	52
4 : 1	180	45
9 : 1	270	30
57 : 1	672	12



d = 1.74 mm

Stress formulas :

Center(A):

$$\sigma_x = A_x p \frac{b^2}{d^2}$$

$$\sigma_y = A_y p \frac{b^2}{d^2}$$

Edge(B):

$$\sigma_x = \nu B_y p \frac{b^2}{d^2}$$

$$\sigma_y = B_y p \frac{b^2}{d^2}$$

Edge(C):

$$\sigma_x = C_x p \frac{b^2}{d^2}$$

$$\sigma_y = \nu C_x p \frac{b^2}{d^2}$$

Coefficients :

a : b	A _x	A _y	B _y	C _x
1 : 1	0,1225	0,1225	0,1900	0,1900
2 : 1	0,1075	0,2175	0,4000	0,0950
3 : 1	0,0950	0,2375	0,4500	0,0500
4 : 1	0,0875	0,2450	0,4700	0,0300
9 : 1	0,0750	0,2500	0,4950	0,0050
57 : 1	0,0750	0,2500	0,4950	0,0010

if we take care of window given size, formula become:

Center(A)

$$\sigma_x = \alpha_x p$$

$$\sigma_y = \alpha_y p$$

Edge(B):

$$\sigma_x = \nu \sigma_y$$

$$\sigma_y = \beta_y p$$

Edge(C):

$$\sigma_x = \chi_x p$$

$$\sigma_y = \nu \sigma_x$$

and coefficient are:

a : b	α _x	α _y	β _y	χ _x
1 : 1	320	320	497	497
2 : 1	141	285	525	125
3 : 1	85	212	401	45
4 : 1	58	164	314	20
9 : 1	22	74	146	1
57 : 1	4	12	24	0

Example of calculation:

a : b = 2 : 1

Δp = 5 bars

σ_x = α_x p = 141*5 = 705 bars so 70.5 MPa

a : b = 3 : 1

Δp = 5 bars

σ_x = α_x p = 85*5 = 425 bars so 42.5 MPa

All coefficients are positive in order to not confuse between Tensile Strength and Compressive Strength when you want to check the window limits. (Compressive Strength >> Tensile Strength)


Table VIII: Mechanical stress in elliptical windows due to a pressure difference Δp.

6.4 Numerical Calculations on Stress Distributions

Finite element calculations on stress distribution and overpressure have been performed using the ABAQUS code supported by the CAD program BRAVO for preparation of the discretization mesh.

- step 1: cooling down of the window to 77 K with a full pressure difference of $\Delta p = 5$ bar (poisson coefficient of steel = 0.3 was used).
- step 2: superposition of CW-gyrotron power distribution

The results are summarized in Table IX and in the Figs 9a,b,c.

	aspect ratio a : b		
	3 : 1	4 : 1	9 : 1
a (mm)	156	180	270
b (mm)	52	45	30
d (mm)	1.74	1.74	1.74
step 1			
$\sigma_{TS,max}$	+42	+34	+15.5
$\sigma_{c,max}$	-42	-34	-15.5
$\sigma_{von Mises,max}$	51	39	17.5
step 2			
$\sigma_{TS,max}$	+41.5	+33.5	+15.5
$\sigma_{c,max}$	-43	-34.5	-16
$\sigma_{von Mises,max}$	51.5	39	16
center			
σ_{max}	111.5	83.5	37
edge			
σ_{max}	-223	-167	-74.5

$\sigma_{TS,max}$ = maximum tensile stress (MPa)

$\sigma_{c,max}$ = maximum compressive stress (MPa)

$\sigma_{von Mises, max}$ = maximum von Mises stress (MPa)

σ_{max} = maximum bending tensile / compressive stress (MPa)
derived from analytical formulas, all edges pinned.

Table IX: Finite element calculations on stress distributions.

The main stress in the window is due to the pressure difference. Since the measured bending tensile strength of HEMEX sapphire is around 500 MPa and the compressive strength is approximately 2800 MPa all stresses are well below the admissible limits. However, for an industrial design, also the stress due to the soldering/brazing has to be taken into account, that strongly depends on the design of the brazing collar.

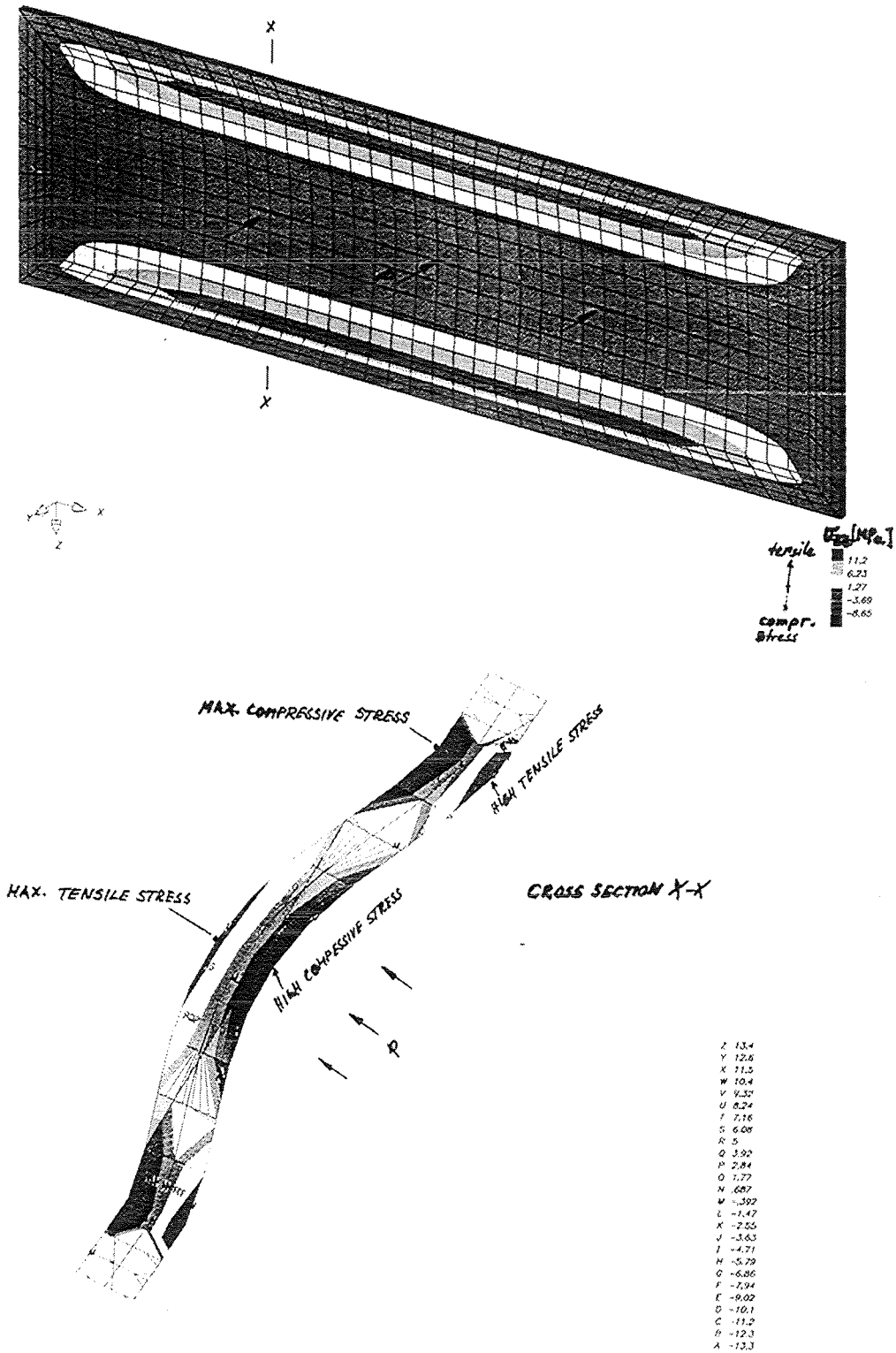


Fig. 9a: Typical calculated stress distribution in a rectangular sapphire window (aspect ratio 4:1) under pressure loading Δp (the deformation is largely scaled for better view).

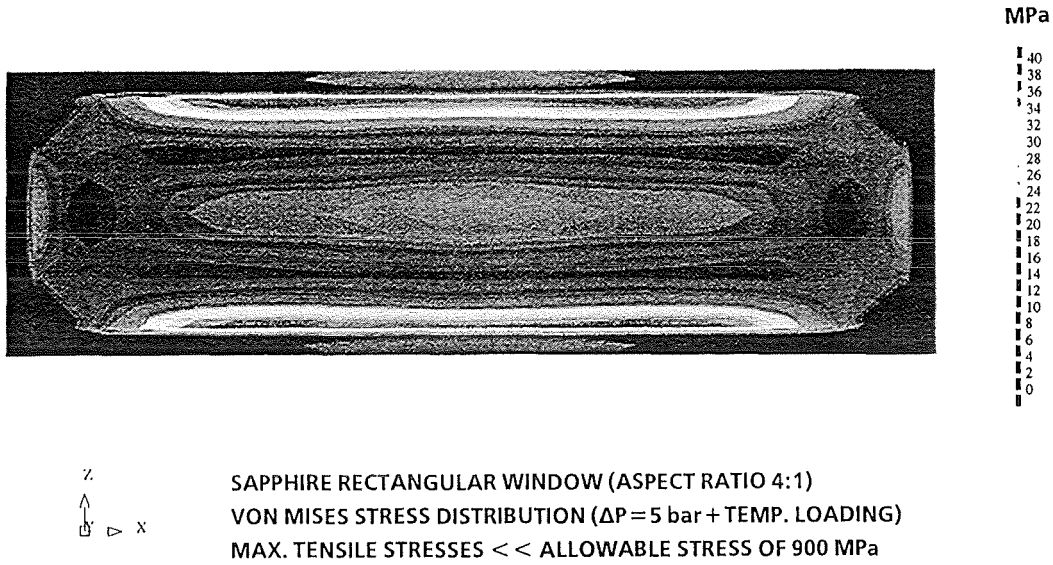


Fig. 9b: Von Mises stress distribution ($\Delta p = 5$ bar + temp. loading) for rectangular sapphire window (aspect ratio 4:1)

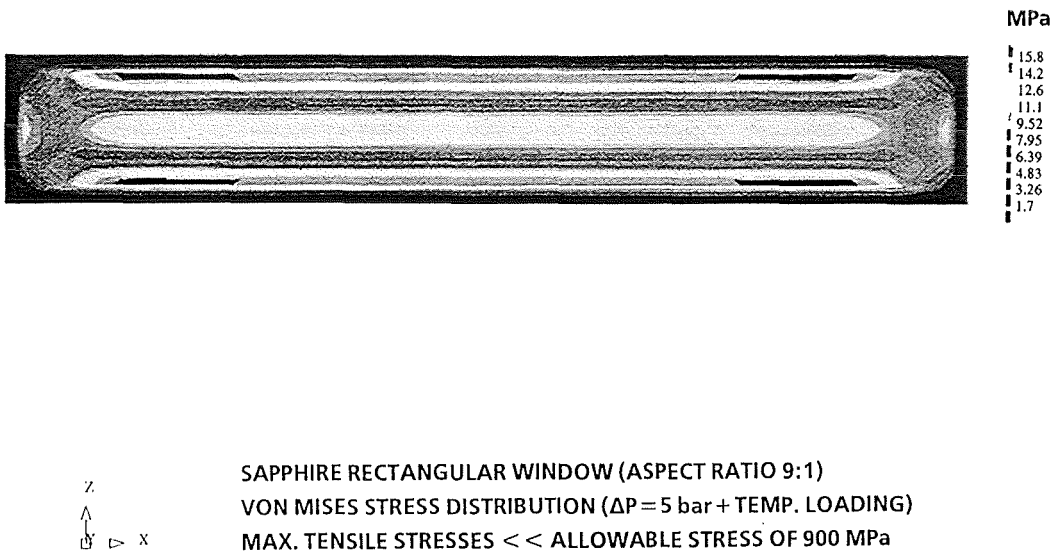


Fig. 9c: Von Mises stress distribution ($\Delta p = 5$ bar + temp. loading) for rectangular sapphire window (aspect ratio 9:1)

Bending stresses during the brazing process can be minimized by brazing a thick back-up ring together with the sapphire disk (Fig. 10).

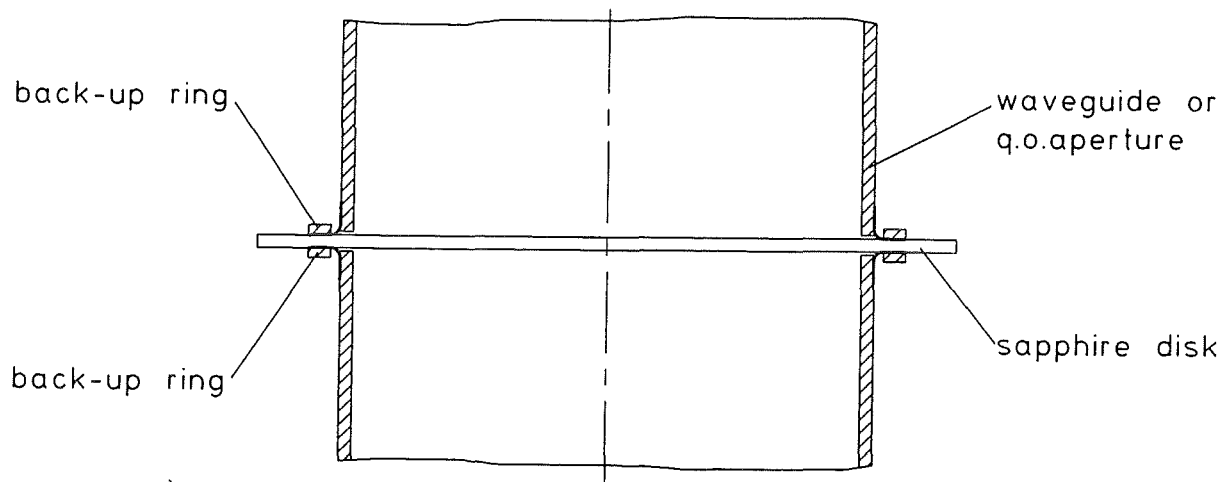


Fig. 10: Face brazing technique employing a back-up ring for bending stress minimization.

6.5 Production and Metallization of Elongated Sapphire Disks

NIFS Nagoya has succeeded in manufacturing large-area elongated sapphire disks in collaboration with Kyocera Corporation. In this process, two new technologies are achieved, firstly, the production of large-size C-cut single crystalline sapphire disks by the edge-defined film-fed growth method and secondly, minimizing distortions of the disk under metallizing and brazing processes. They have manufactured a C-cut elongated sapphire disk with the effective area of 65 x 240 mm². Bending along the longer axis, which happened during metallizing and brazing processes, was minimized up to about 20 micrometer by brazing a thick alumina back-up ring together with the sapphire disk. The disk is equipped with a Kovar flange.

7. Subtask 3: Assessment and design of a non-cryogenic, large-aspect-ratio rectangular, water-cooled single disk torus window system.

Summary

As an alternative to the distributed window concept under development by the US Home Team, the EU Home Team considers a high-aspect-ratio rectangular waveguide window inclined at the Brewster angle. This broadband concept will use water edge cooling of a single disk made out of Au-doped silicon or PACVD diamond. The window assembly consists of an open-ended corrugated circular HE_{11} waveguide, radiating into a dog-leg configuration consisting of a defocusing and a focusing reflector which generate the highly elongated HE_{11} mode of a corrugated rectangular (200 mm x 12 mm) waveguide that houses the Brewster window. The reflectors are contained in an evacuated box. Behind the window, the back conversion to the circular HE_{11} waveguide is achieved by applying the reflectors in the inversed sequence. The final design is presented. The total losses of the assembly (7.3 %) can be reduced to approximately 3 % by using periodically rippled wall mode converters to generate the 90 % HE_{11} /10 % HE_{12} (in phase) mode mixture for optimum coupling to the free-space Gaussian mode.

Quasi-optical methods have been used in order to reduce the transition length to get the large-aspect-ratio elliptical HE_{11} mode .

Finite element calculations on the temperature and stress distributions at 170 GHz and $\Delta p=5$ bar show that Au-doped silicon ($\tan\delta \approx 1/f$) and PACVD diamond ($\tan\delta \approx \text{const}$) are possible candidates. Diamond is preferable since there is no danger of enhanced losses due to thermal excitation of charge carriers at temperatures higher than 350 K.

Nevertheless, a conventional circular, water cooled diamond window would have a much simpler mechanical structure compared to the present large-aspect ratio rectangular window. Additionally, there would be much lower losses.

7.1. Concept of Large-Aspect-Ratio Brewster Window

This concept uses water edge cooling of a single disk made out of Au-doped silicon or CVD diamond (Fig. 11). The Brewster angle for reflection free, broadband transmission is given by

$$\theta_{\text{Brew}} = \arctan \sqrt{\epsilon_r'}$$

Silicon (Au-doped)	$\epsilon_r' = 11.7$	$\theta_{\text{Brew}} = 73.7^\circ$
Sapphire	$\epsilon_r' = 9.4$	$\theta_{\text{Brew}} = 71.9^\circ$
Diamond	$\epsilon_r' = 5.7$	$\theta_{\text{Brew}} = 67.3^\circ$

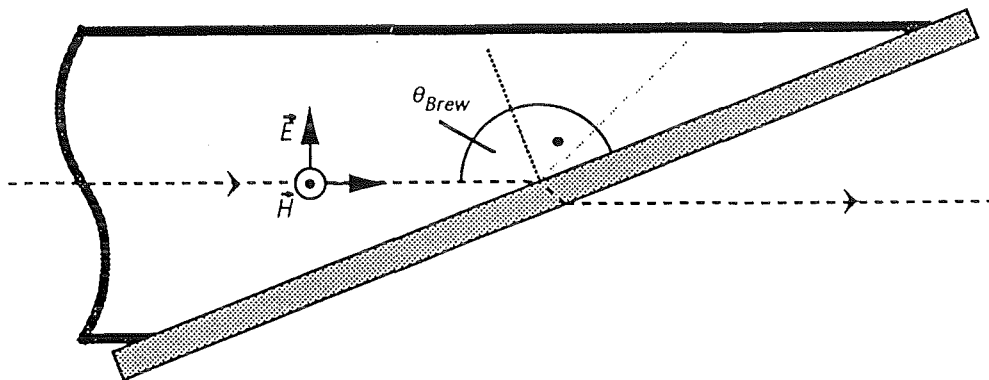


Fig. 11: Principle of Brewster Window.

In case that the high aspect ratio window disk cannot be manufactured in one piece, two or more parts can be brazed together using thin metal vanes perpendicular to the E-field (as in the distributed window) which are parallel to the short sides of the waveguide.

The principle of the window assembly is shown in Fig. 12. It consists of:

- open-ended corrugated circular HE_{11} waveguide,
- quasi-optical dog-leg configuration consisting of a pair of reflectors (in the x-z plane one is defocusing the other focusing) which generate the highly elongated HE_{11} mode of a rectangular (200 mm x 12 mm) corrugated waveguide, that houses the Brewster Window. The reflectors are contained in an evacuated mirror box.
- inverse rectangular to circular HE_{11} back transition.

The different window components are described in the following chapters.

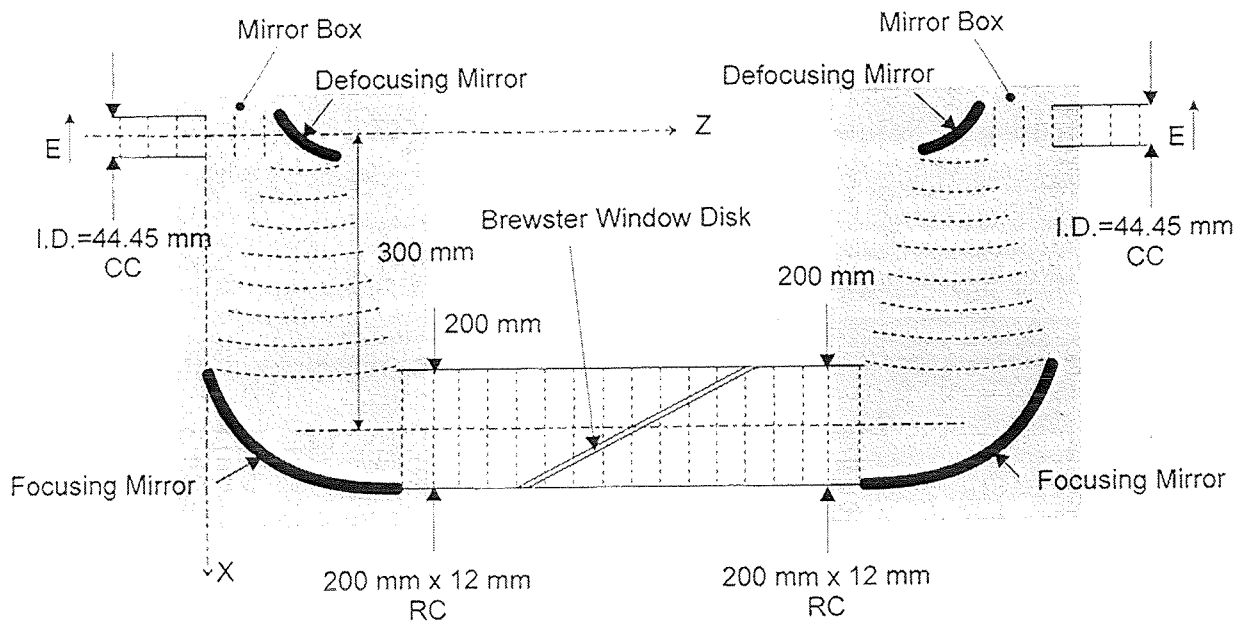


Fig. 12: Principle of large-aspect-ratio Brewster angle window.

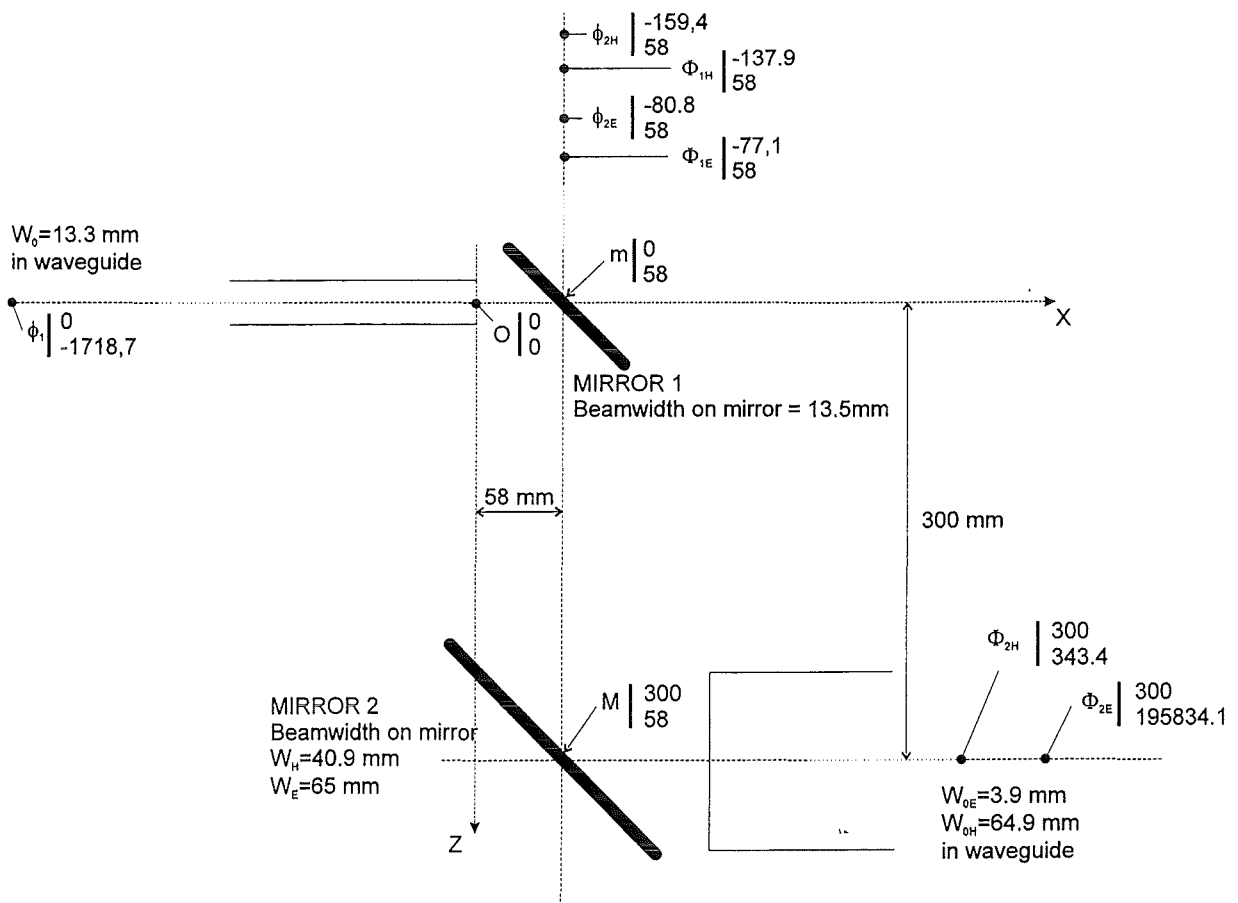


Fig. 13: Geometry of dog-leg configuration of two reflectors.

7.2 Quasi-optical Circular Corrugated (CC) to Rectangular Corrugated (RC) Waveguide Transition

The length of a nonlinear H-plane taper to reduce the distance of the isotropic impedance surfaces (smooth) from e.g. 41 mm to 12 mm with a spurious mode excitation of lower than - 20 dB was calculated using the FZK taper contour synthesis code to be only approximately 0.6 m.

However, the predicted length of a nonlinear E-plane taper to increase the distance of the anisotropic impedance surface (corrugated) from 41 to 200 mm has a non-acceptable length of more than 10 m. So quasi-optical methods must be used in order to reduce the transition length to get the large-aspect-ratio elliptical HE_{11} mode. The dog-leg configuration of a defocusing and a focusing mirror was optimized using a geometric-optics code. the geometrical data are summarized in Fig. 13. For broadband performance, the optics must be confocal.

7.3 Additional Losses

The realistic ohmic losses of the combination of 4 E-plane reflectors are 1.3 %. Much higher are the coupling losses from the HE_{11} waveguide modes to the free space Gaussian modes. The 4 coupling junctions together introduce approximately 6 % losses, so that the total losses amount to 7.3 %. However, a 90 % HE_{11} /10 % HE_{12} (in phase) mixture optimally couples to the Gaussian beam leading to only about 1.6 % coupling losses, that means to 3 % total losses. Such mode mixtures can be generated by periodically rippled wall mode converters. [17]

7.4 Large-aspect Ratio Rectangular Brewster Window (57:1)

Numerical calculations at 170 GHz on the temperature distribution have been performed using the finite element code ABAQUS supported by the pre-processor code FEMGEN for preparation of the discretization mesh. The assumed window disk has an aperture of

$$680 \text{ mm} \times 12 \text{ mm} \text{ (Brewster angle } \approx 73 \text{ degrees)}$$

with a 25 mm rim for water edge cooling at 293 K. The results are summarized in Table X and Fig. 14.

Material	thickness d(mm)	$\tan\delta$	ϵ_r	k (W/mK)	P_{\max} (MW)	T_{\max}/T_{\min} (K)	Q_{absorbed} (W)
Sapphire	1.74	1.778E-4	9.4	48	0.05	395/294	414
Silicon	1.80	0.1 E-4	11.7	148	1.76	394/294	850
Silicon	1.80	0.1 E-4	11.7	148	1.00	325/293	355
Diamond	1.85	0.5 E-4	5.7	900	1.76	364/294	1623
Diamond	1.85	0.5 E-4	5.7	900	1.00	333/293	922

Table X: Power transmission capability of different large aspect-ratio rectangular windows (aperture: 680 mm x 12 mm) with water edge cooling.

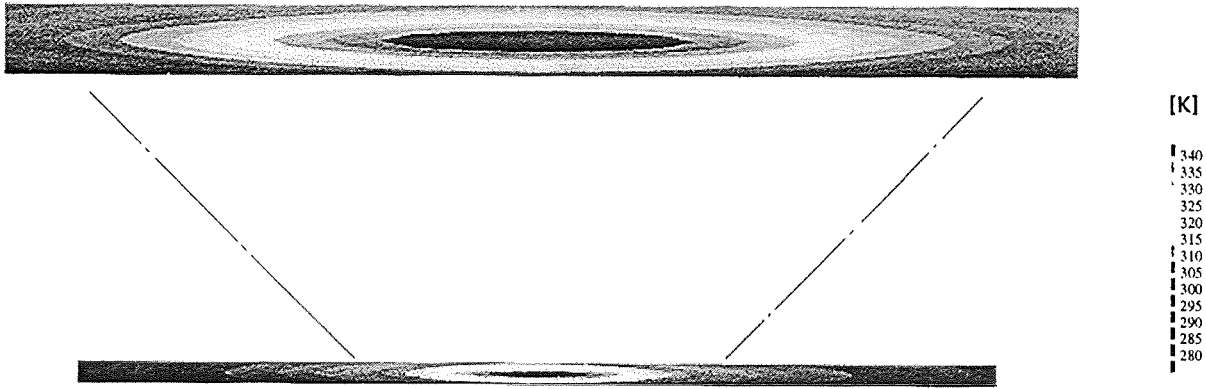


Fig. 14: Temperature distribution for large aspect ratio (58:1) rectangular silicon window ($P = 1.75$ MW, 140 GHz, Gaussian).

The calculations evidently that sapphire cannot be used.

Au-doped silicon ($\tan\delta \approx 1/f$) and CVD diamond ($\tan\delta \approx 1/\sqrt{f}$ and $\approx \text{const}$ as function of temperature) are possible candidates. The temperature dependence of different silicon and diamond grades are presented in Fig. 15 and 16. Both materials are suitable for Brewster window since they are isotropic.

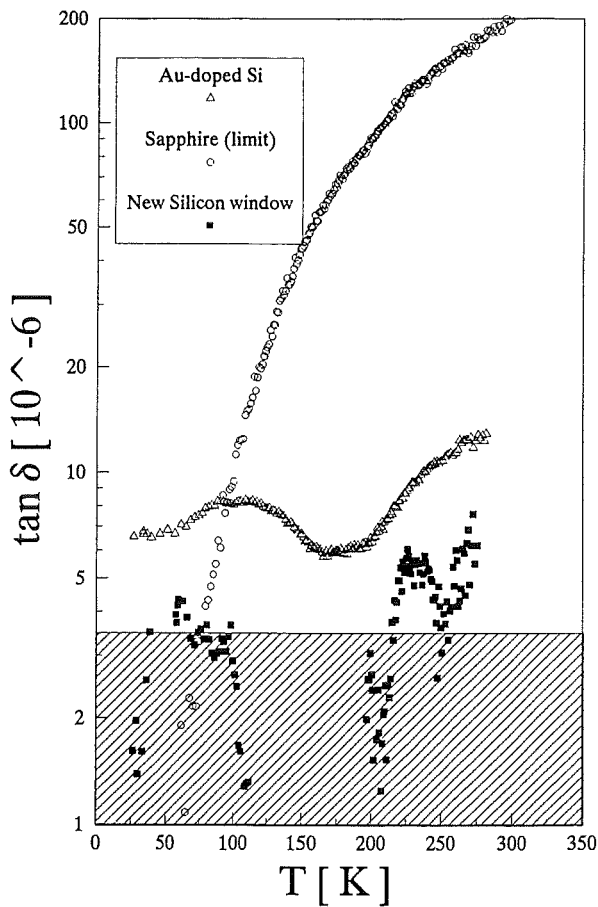


Fig. 15: Temperature dependence of dielectric loss at 145 GHz for sapphire and Au-doped silicon.

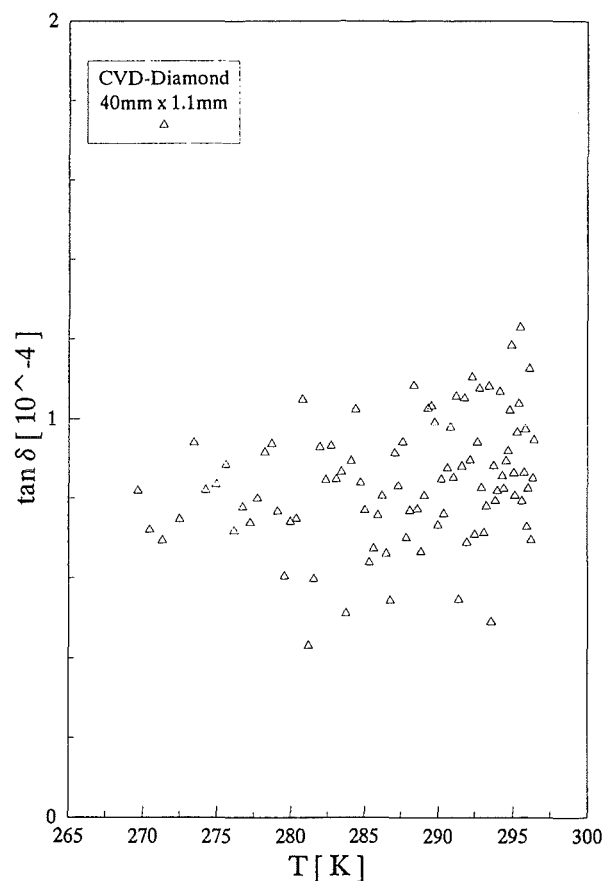


Fig. 16: Temperature dependence of dielectric loss at 145 GHz for PCVD diamond.

Finite element computations and calculations using the analytical formulas of Tables VII and VIII show clearly that all stresses are very well below the admissible limits.

7.5 Conclusions

Large-aspect ratio rectangular Brewster-angle windows in a corrugated 200 mm x 12 mm rectangular HE_{11} waveguide are feasible for 170 GHz, CW operation if one utilizes Au-doped silicon or PACVD diamond window disks. For silicon ($\theta_{\text{Brew}} = 73.7^\circ$) the window aperture could be 684 mm x 12 mm (57:1) and for diamond ($\theta_{\text{Brew}} = 67.3^\circ$) it would be 478 mm x 12 mm (40:1). Diamond is preferable since there is no danger of enhanced losses due to thermal excitation of charge carriers at temperatures higher than 350 K. According to DeBeers Company (UK) PACVD diamond can be already manufactured in a length of 140 mm and a thickness of 2.1 mm, so that the complete window disk (520 mm x 60 mm) including the rim for water cooling would consist of 4 rectangular parts (130 mm x 40 mm) brazed together using thin metal vanes parallel to the short sides. Recent measurements at FZK on a new PACVD diamond specimen revealed a reduced loss tangent value of $\tan \delta = 0.2 \text{ E-}4$ so that conventional circular windows become feasible. A conventional circular diamond window would have a much simpler mechanical structure compared to the present large-aspect ratio rectangular window. Additionally, there would be much lower losses.

8. Subtask 4: Optimization and design of a liquid neon edge cooled single disk sapphire window for 1 MW, CW operation.

Summary

The FZK LNe window design is based on a single circular sapphire disk of 140 mm diameter and 1.74 mm thickness ($6 \lambda/2$) in a short cylindrical waveguide structure of about 60 to 90 mm diameter. The microwave energy absorbed in the window disk is removed by nucleate boiling liquid neon at atmospheric pressure (27.15 K) in a rim around the edge of the disk ("bath" cooling). Using the measured power absorption factor of $\tan\delta = 1.48 \cdot 10^{-11} (f/\text{GHz}) \cdot (T/\text{K})^2$ for Ti-doped sapphire and the relatively low value ($\approx 1500 \text{ W/mK}$) for the thermal conductivity, recently measured at CEA Cadarache for HEMEX grade quality (Crystal Systems), the maximum calculated CW power transmission for a Gaussian/ HE_{11} -power distribution is 2.8 MW, 2.3 MW and 1.8 MW at 140 GHz, 170 GHz and 220 GHz, respectively.

At 1 MW, 170 GHz, CW the power absorbed by the window disk is 67 W and the maximum and minimum temperatures would be $T_{\max} = 34 \text{ K}$ and $T_{\min} = 29 \text{ K}$ (for a diameter of 90 mm), respectively.

Computations and design studies on realistic window assemblies have been done. Special care has to be taken in order to minimize the static liquid neon consumption.

The closed-cycle neon refrigeration system "Philips Cryogenerator PH 110" (refrigeration capacity: 150 W) available at FZK Karlsruhe will be used for first experimental tests on such a liquid neon cooled single-disk sapphire window at 118 GHz, 0.5 MW, 210 s using the European TTE gyrotron at CEA Cadarache.

8.1. Concept of Liquid Neon Edge Cooled Single Disk Sapphire Window

Lowering the temperature of a sapphire window to $T = 27 - 30$ K results in a strong reduction of $\tan\delta$ and permits operation in the range of maximum thermal conductivity (Fig. 17) [18]. For heat removal at these temperatures one can use a liquid neon bath at atmospheric pressure. Neon can be simply liquefied by making use of an available flow of cold He gas.

The FZK LNe window design is based on a single circular disk of 140 mm diameter and 1.74 mm thickness ($6 \lambda/2$) in a short cylindrical waveguide structure of about 90 mm diameter (Fig. 7). The microwave energy absorbed in the window disk is removed by nucleate boiling liquid neon at atmospheric pressure (27.15 K) in a rim around the edge of the disk.

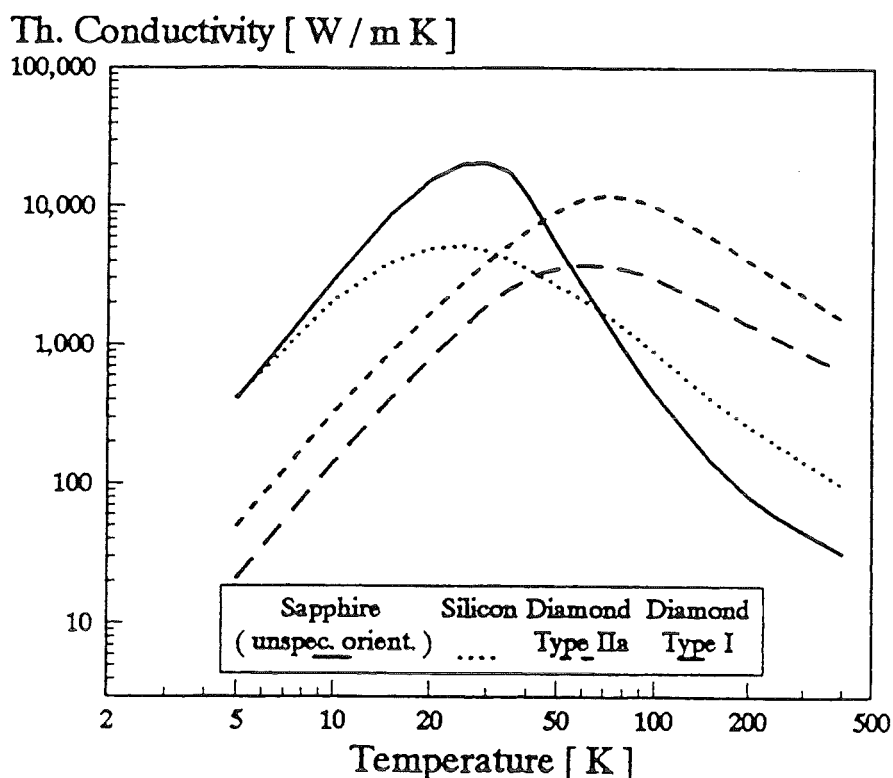


Fig. 17.: Thermal conductivity of sapphire, silicon and diamond [18].

8.2. Calculation of Power Transmission Capabiliy

Optimization and design calculations on a liquid neon edge cooled single disk sapphire window for high-power CW millimeter waves in the frequency range between 140 and 220 GHz have been performed using the finite element code ABAQUS supported by the pre-processor code FEMGEN for preparation of the discretization mesh.

Using the measured power absorption factor of $\tan\delta = 1.48 \cdot 10^{-11} (f/\text{GHz}) \cdot (T/\text{K})^2$ (pessimistic value) (Fig. 18) for Ti-doped sapphire and the relatively low value (≈ 1500 W/mK) for the thermal conductivity, recently measured at CEA Cadarache for HEMEX grade quality (Fig. 19) [19], the maximum calculated CW power transmission for a Gaussian / HE_{11} -power distribution is 2.8 MW, 2.3 MW and 1.8 MW at 140 GHz, 170 GHz and 220 GHz, respectively. The numerical results are summarized in Fig. 20 and Table XI.

That means, that lowering the operational temperature from 77 K to about 30 K increases the power capability by a factor of about 5.6, allowing even 2 MW windows at 170 GHz. However, in contrast to liquid nitrogen cooled windows, liquid neon cooled windows always must be operated in an evacuated waveguide in order to avoid freezing. In the case of the torus window LN₂ cryotrapping in a pumping waveguide coldtrap on the torus side should pump the dust in the waveguide. There is no danger of tritium condensation since this happens at lower temperature (20 K).

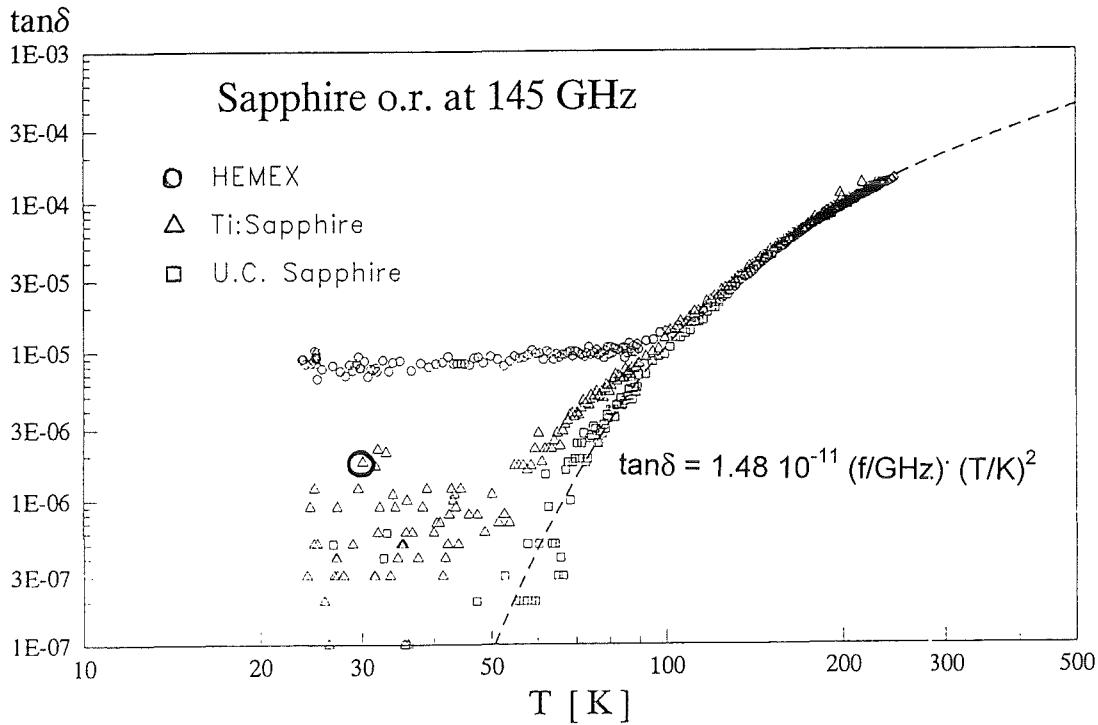


Fig. 18: Temperature dependence of dielectric loss of various sapphire grades.

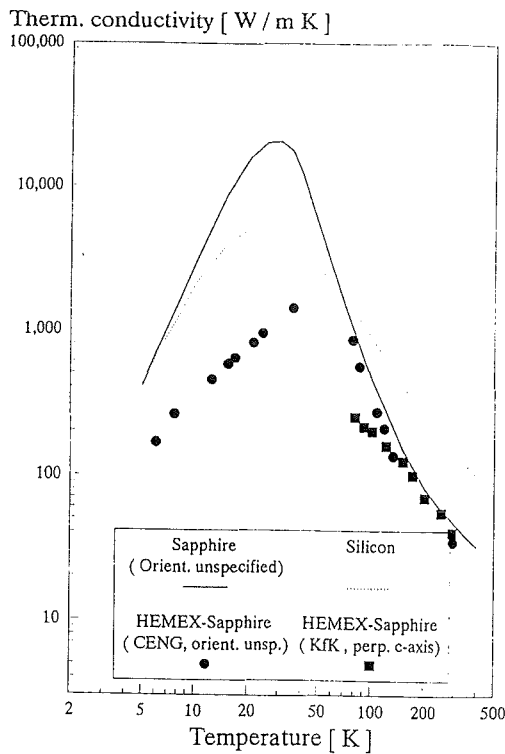


Fig. 19: Recommended thermal conductivity data [18] compared with measurements [19].

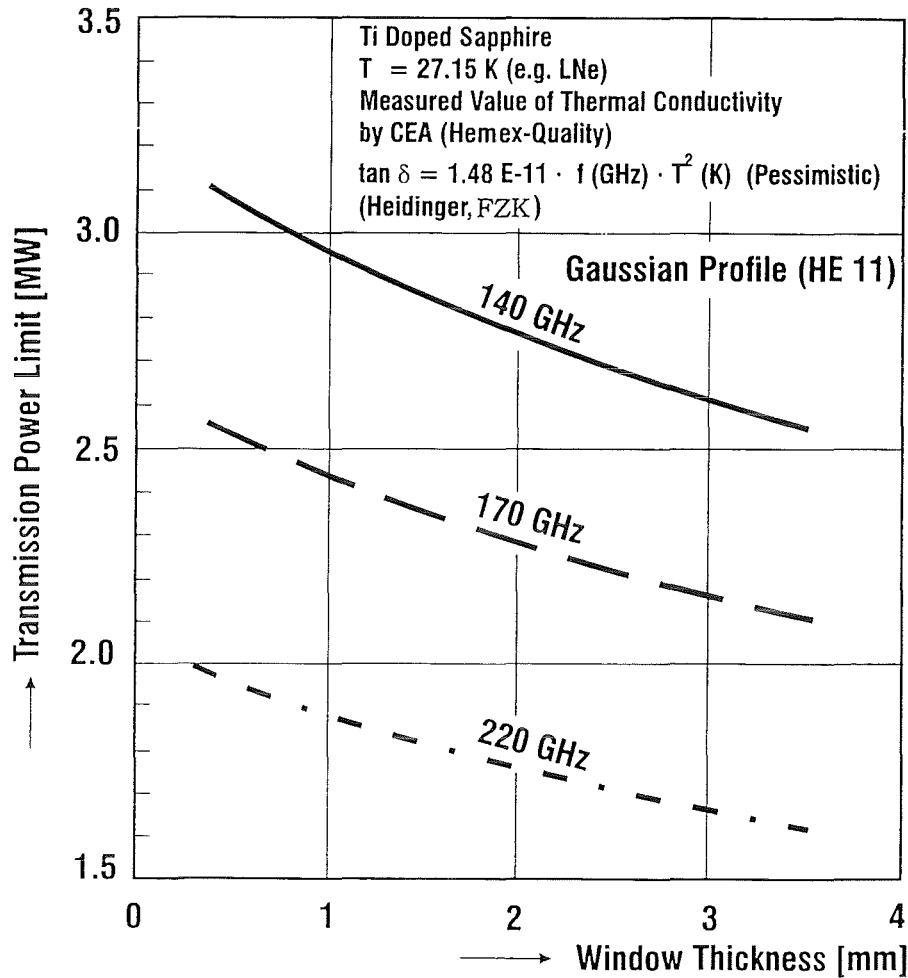


Fig. 20: Maximum transmission power as a function of window thickness.

8.3 Preparation of an Experimental Validation (T245/6)

The following Table XI summarizes numerical results of computations on the thermal window behavior for different frequencies and power using a Gaussian/HE₁₁-power distribution.

f (GHz)	thickness d (mm)	P (MW)	T_{\max}/T_{\min} (K)	Q_{absorbed} (W)
118	2.09	1.0 (0.5)	33 (30) / 27	58 (29)
140	1.74	1.0	33 / 27	55
140	1.74	2.6 (max.)	48 / 30	241
170	1.72	1.0	34 / 29	67
170	1.72	2.1 (max.)	47 / 30	231

Table XI: Finite element calculations for various LNe-cooled sapphire windows.

At 0.5 MW, 118 GHz, 210 s operation the power absorbed by the window disk is 29 W and the maximum and minimum temperatures would be $T_{\max} = 30 \text{ K}$ and $T_{\min} = 27 \text{ K}$, respectively.

The closed-cycle neon refrigeration system "Philips Cryogenerator PH 110" (refrigeration capacity: 150 W) available at FZK Karlsruhe could be used for first experimental tests on such a window system. However, since this cryogenerator is relatively bulky, an approximately 4 m long LNe-transmission line to the window cryostat was purchased from cryo-industries and is now available at FZK. Test runs of the cryogenerator were successful.

The window tests at CEA Cadarache could be performed employing an improved version of the TTE 118 GHz gyrotron window assembly (Fig. 21) in an evacuated HE_{11} waveguide run (waveguide diameter = 63.5 mm). Special care has to be taken in order to minimize the static liquid neon consumption. The commissioning of the window assembly is under way.

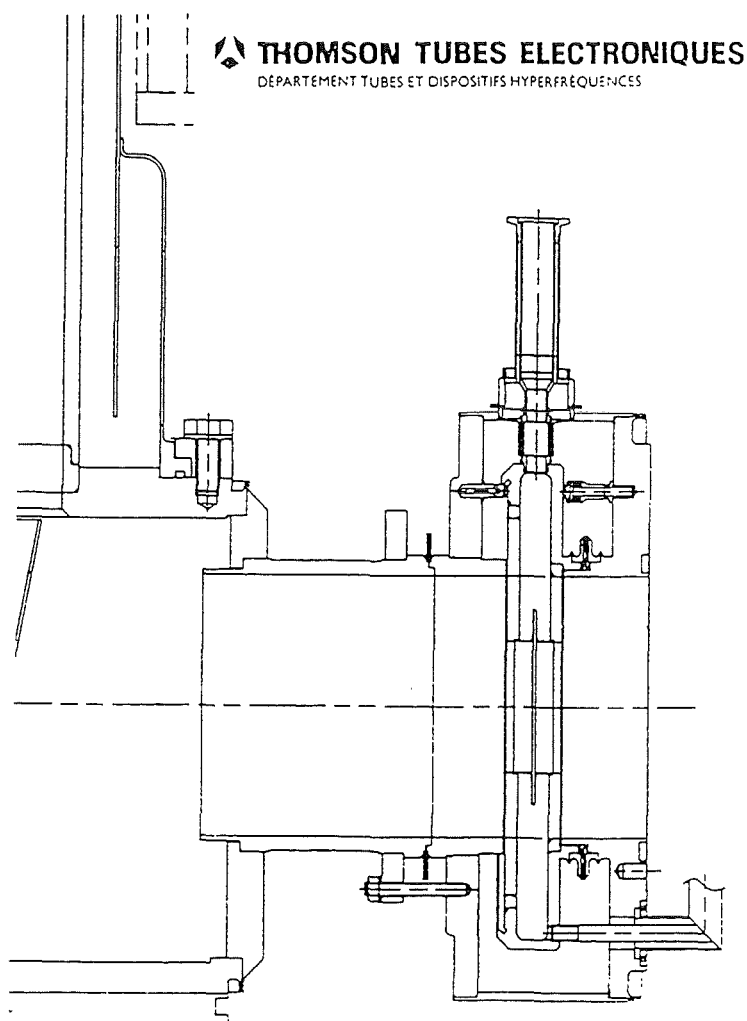


Fig. 21: Schematic drawing of the LN_2 -edge-cooled single-disk sapphire window of the European quasi-continuous 210 s/500 kW 118 GHz gyrotron oscillator manufactured by TTE.

References

- [1] Norajitra, P., Häfner, H.E., Thumm, M., 1995, Alternatives for edge cooled single disk windows with 1 MW transmission power, Conf. Digest 20th International Conference on Infrared and Millimeter Waves, Lake Buena Vista (Orlando), USA, pp. 475-476.
- [2] Häfner, H.E., Norajitra, P., Müller, K., Thumm, M., 1994, Conceptual Design and Thermodynamics Study of Cryogenically Edge Cooled Windows for ECR Plasma Heating, 18th SOFT, Karlsruhe, Germany, Fus. Tech. Vol.1, pp. 505-508.
- [3] Häfner, H.E., Bojarsky, E., Heckert, K., Norajitra, P., Reiser, H., 1994, Liquid nitrogen cooled window for high frequency plasma heating. Journal of Nuclear Materials, **212-215**, pp. 1035-1038.
- [4] Häfner, H.E., Heckert, K., Norajitra, P., Vouriot, R., Hofmann, A., Münch, N., Nickel, H.-U., Thumm, M., Erckmann, V., 1994, Investigations of liquid nitrogen cooled windows for high power millimeter wave transmission, Conf. Digest 19th Int. Conf. on Infrared and Millimeter Waves, Sendai, JSAP Catalog No.: AP 941228, pp. 281-282.
- [5] Saitoh, Y., Itoh, K., Yoshiyuki, T., Ebisawa, K., Yokokura, K., Nagashima, T., Yamamoto, T., 1992, Cryogenic window for millimeter-wave transmission, Fusion Technology 1992, eds. C. Ferro, M. Gasparotto, H. Knoepfel (Elsevier Science Publishers B.V. 1992), pp. 632-636.
- [6] Kasugai, A., Yokokura, K., Sakamoto, K., Tsuneoka, M., Yamamoto, T., Imai, T., Saito, Y., Ito, K. Yoshiyuki, T., Ebisawa, K., 1994, High power tests of the cryogenic window for millimeter wave. Conf. Digest 19th Int. Conf. on Infrared and Millimeter Waves, Sendai, JSAP Catalog No.: AP 941228, pp. 295-296.
- [7] Pain, M., Berger-By, G., Capitain, J.J., Crenn, J.P., Smits, F., Tonon, G., 1992, The 110 GHz electron cyclotron heating and current drive system for Tore Supra, Proc. 8th Joint Workshop on Electron Cyclotron Emission and Electron Cyclotron Resonance Heating (EC-8), Gut Ising, Germany, Vol II, pp. 523-530.
- [8] Fix, A.S., Sushilin, P.B., 1993, Calculation and experimental investigation of cryogenic window, Proc. 5th Russian-German Meeting on ECRH and Gyrotrons, Karlsruhe, pp. 389-392 and, 1994, Proc. 6th Russian-German Meeting on ECRH and Gyrotrons, Moscow, 1994, Vol. 2, pp. 244-247.
- [9] Garin, P., Bon-Mardion, G., Pain, M., Heidinger, R., Thumm, M., Dubrovin, A., Giguet, É., Tran, C., 1995, Cryogenically cooled window: A new step toward gyrotron CW operation, Conf. Digest 20th International Conference on Infrared and Millimeter Waves, Lake Buena Vista (Orlando), USA, pp. 271-272.
- [10] Shimozuma, T., Sato, M., Takita, Y., Kubo, S., Idei, H., Ohkubo, K., Watari, T., Morimoto, S., Tajima, K., 1995, Development of elongated vacuum windows for high power CW millimeter waves, Conf. Digest 20th International Conference on Infrared and Millimeter Waves, Lake Buena Vista (Orlando), USA, pp. 273-274.
- [11] Moeller, C.P., Doane, J.L., DiMartino, M., 1994, A vacuum window for a 1 MW CW 110 GHz gyrotron, Conf. Digest 19th Int. Conf. on Infrared and Millimeter Waves, Sendai, Conf. Digest 19th Int. Conf. on Infrared and Millimeter Waves, Sendai, JSAP Catalog No.: AP 941228, 279-280.
- [12] Heidinger, R., 1994, Dielectric property measurements on CVD diamond grades for advanced gyrotron windows, Conf. Digest 19th Int. Conf. on Infrared and Millimeter Waves, Sendai, JSAP Catalog No.: AP 941228, pp. 277-278.
- [13] Parshin, V.V., Heidinger, R., Andreev, B.A., Gusev, A.V., Shmagin, V.B., 1995, Silicon with extra low losses for megawatt output gyrotron windows, Conf. Digest 20th International Conference on Infrared and Millimeter Waves, Lake Buena Vista (Orlando), USA, pp. 22-23.
- [14] Dodin, E.P., Parshin, V.V., Shastin, V.N., 1995, Effect of absorption saturation in silicon in strong electromagnetic fields of mm-wavelength range, Conf. Digest 20th International Conference on Infrared and Millimeter Waves, Lake Buena Vista (Orlando), USA, pp. 28-29.

- [15] Heidinger, R., Link, G., 1995, The mm-wave absorption in sapphire and its description by the 2-phonon model, Conf. Digest 20th International Conference on Infrared and Millimeter Waves, Lake Buena Vista (Orlando), USA, pp. 16-17.
- [16] Heidinger, R., 1994, Dielectric measurements on sapphire for electron wave systems, Journals of Nuclear Materials 212-215, pp. 1101-1106.
- [17] Graubner, T., Kasperek, W., Kumric, H., 1993, Optimization between HE_{11} -Waveguide mode and Gaussian beam, Conf. Digest 18th International Conference on Infrared and Millimeter Waves, Colchester, Essex, SPIE Proc. Vol. 2104, pp. 477-478.
- [18] Touloukain, et al., 1970, Thermophysical properties of matter, Vol.2, IFI/Plenum, New-York-Washington.
- [19] Cadeau, M., Rouillon, H., Marcou, A., Novembre 1993, Mesures de Conductivite Thermique du Saphir, CEA-CENG/DRFMC, Note SBT/CT/93-47.